To the Graduate Council:

I am submitting herewith a thesis written by Kang Lee entitled "An Experimental Method for Developing J-R Curves from Load Versus Crack Length Records." I have examined the final copy of this thesis for form and content and recommend that it be accepted in partial fulfillment of the requirements for the degree of Master of Science, with a major in Engineering Science.

J. D. Landes

J. D. Landes, Major Professor

We have read this thesis
and recommend its acceptance:

Thomas G Carley

Wayman E. Scott

Accepted for the Council:

C W Minkel

Vice Provost
and Dean of The Graduate School

AN EXPERIMENTAL METHOD FOR DEVELOPING J-R CURVES FROM LOAD VERSUS CRACK LENGTH RECORDS

A Thesis
Presented for the
Master of Science
Degree
The University of Tennessee, Knoxville

Kang Lee

August 1990

ACKNOWLEGMENT

In the course of this thesis research, several people have assisted me generously.

First of all, I would like to express my special thanks to Dr. J. D. Landes. As my advisor, Dr. Landes suggested this research topic and offered me a number of test records for the research. His consistent advice, criticism and encouragement were the guide leading me toward the completion of the research. After the first draft of the thesis was finished, Dr. Landes reviewed the whole manuscript and suggested many corrections and improvements.

Also I would like to thank Dr. T. G. Carley and Dr. W. E. Scott, who served as my committee members, for their consultation, criticism and encouragement.

Finally, I would like to thank my uncle Dr. C. W. Lee, my aunt Jean Lee and my wife Yuying Yang. I am most fortunate to have such a wonderful uncle, aunt and wife to offer their continued support, encouragement, especially my uncle's advice was always the source of power in my progress.

With their help I was able to complete the thesis research, which otherwise would be impossible. Whatever errors remained in my work, however, are solely my responsibility.

ABSTRACT

The LMN normalization method introduced by Landes et al. has been used successfully to develop J-R curves from load versus displacement records without crack length measurement. This method uses a so-called LMN function to describe the plastic deformation curve, which gives an unique relationship between load, plastic displacement and crack length. It not only eliminates the need for crack length monitoring equipment, therefore providing a method for more easily conducting and evaluating J-R curve tests; but it could be useful for tests conducted under some special conditions such as in hot cell testing or dynamic testing, or even in a facility with limited instrumentation.

One proposed application of the LMN normalization method is for developing J-R curves from load versus crack length records where displacement measurements cannot be made. This could be important, for example for conducting and analyzing a J-R curve test in a hot cell. In order to do this some additional details of the method must be developed. The key in such a case is how to determine the LMN function for each test specimen. This study tries to use the material flow properties to predict some calibration points on the plastic deformation curve for the determination of the LMN function. Three approaches are proposed. These are applied to different test specimens which include a 10 to 1 difference in size and several different metallic materials. These tests were conducted and analyzed previously by the elastic compliance method and also

analyzed by the LMN normalization method from records where both load and displacement were available. The new results are compared with those from both earlier analyses.

This study describes the development of the new features of the three approaches and shows examples of how well they work. One approach in particular, the power law approach, is found to work best. The results from this approach are found to be consistent with those from the earlier analyses which use the compliance and complete normalization methods. Finally the use of the new approaches for the ASTM J-R curve test is discussed.

TABLE OF CONTENTS

Section . . . Page

1. INTRODUCTION 1

2. BACKGROUND ON THE NEW APPROACHES 6

2.1 The ASTM Standard Test Method, E813 and E1152, for Developing J_{Ic} Values and J-R Curves 7

2.2 The LMN Normalization Method 14

3. DEVELOPING J-R CURVES FROM LOAD VERSUS CRACK LENGTH RECORDS 24

3.1 Introduction 24

3.2 Using the "Handbook" Method to Obtain the Beginning Calibration Points 25

3.3 Using an Empirical Formula to Obtain the Beginning Calibration Points 33

3.4 Using a Power Law Assumption to Obtain the Beginning Calibration Points 38

3.5 The Determination of LMN Function and The Evaluation of J 49

4. APPLICATION RESULTS, DISCUSSION AND CONCLUSIONS. . 51

4.1 Application Results 51

4.2 Discussion and Conclusions 55

BIBLIOGRAPHY 59

APPENDIX 66

VITA 90

LIST OF FIGURES

Figures Page

Fig. 1 A Typical J-R Curve from Elastic Compliance Method . . . 13

Fig. 2 Schematic of Normalized Load Versus Plastic Displacement Curve 18

Fig. 3 Schematic of Calibration Points for LMN Function Fit . . 20

Fig. 4 Normalized Load Versus Plastic Displacement Showing Fixed Intermediate Calibration Point 21

Fig. 5 The Beginning and Final Calibration Points Determined from the Handbook Approach for Specimen A508-24 29

Fig. 6 The Beginning and Final Calibration Points Determined from the Handbook Approach for Specimen A508-25 29

Fig. 7 The Beginning and Final Calibration Points Determined from the Handbook Approach for Specimen A508- 6 30

Fig. 8 The Beginning and Final Calibration Points Determined from the Handbook Approach for Specimen A508- 1 30

Fig. 9 The Beginning and Final Calibration Points Determined from the Handbook Approach for Specimen A533-75 31

Figures | Page

Fig. 10 The Beginning and Final Calibration Points Determined from the Handbook Approach for Specimen A533-76 31

Fig. 11 The Beginning and Final Calibration Points Determined from the Handbook Approach for Specimen HSLA-34 32

Fig. 12 The Beginning and Final Calibration Points Determined from the Handbook Approach for Specimen HSLA-36 32

Fig. 13 The Beginning and Final Calibration Points Determined from the Empirical formula Approach for Specimen A508-24 35

Fig. 14 The Beginning and Final Calibration Points Determined from the Empirical formula Approach for Specimen A508-1 35

Fig. 15 The Beginning and Final Calibration Points Determined from the Empirical formula Approach for Specimen A106-18 36

Fig. 16 The Beginning and Final Calibration Points Determined from the Empirical formula Approach for Specimen A533-76 36

Fig. 17 The Beginning and Final Calibration Points Determined from the Empirical formula Approach for Specimen HSLA-34 37

Figures Page

Fig. 18 The Beginning and Final Calibration Points Determined from the Empirical formula Approach for Specimen HY80-10 37

Fig. 19 The Beginning and Final Calibration Points Determined from the Power Law Approach for Specimen A508-33 41

Fig. 20 The Beginning and Final Calibration Points Determined from the Power Law Approach for Specimen A508-24 41

Fig. 21 The Beginning and Final Calibration Points Determined from the Power Law Approach for Specimen A508- 6 42

Fig. 22 The Beginning and Final Calibration Points Determined from the Power Law Approach for Specimen A508- 1 42

Fig. 23 The Beginning and Final Calibration Points Determined from the Power Law Approach for Specimen A106-17 43

Fig. 24 The Beginning and Final Calibration Points Determined from the Power Law Approach for Specimen A106-18 43

Fig. 25 The Beginning and Final Calibration Points Determined from the Power Law Approach for Specimen A533-71 44

Figures Page

Fig. 26 The Beginning and Final Calibration Points Determined from the Power Law Approach for Specimen A533-76 44

Fig. 27 The Beginning and Final Calibration Points Determined from the Power Law Approach for Specimen HSLA-35 45

Fig. 28 The Beginning and Final Calibration Points Determined from the Power Law Approach for Specimen HSLA-36 45

Fig. 29 The Beginning and Final Calibration Points Determined from the Power Law Approach for Specimen HY80-10 46

Fig. 30 The Beginning and Final Calibration Points Determined from the Power Law Approach for Specimen HY80-11 46

Fig. 31 The Quadratic Polynomial Fitting Result For μ in Eq(3.12) Versus σ_y 48

Fig. 32 J-R Curve from Handbook Approach for Specimen A508-24 67

Fig. 33 J-R Curve from Handbook Approach for Specimen A508- 6 68

Fig. 34 J-R Curve from Handbook Approach for Specimen A106-17 69

Fig. 35 J-R Curve from Empirical Formula Approach for Specimen A508-24 70

Figures | | Page
Fig. 36 J-R Curve from Empirical Formula Approach for Specimen A508- 6 71
Fig. 37 J-R Curve from Empirical Formula Approach for Specimen A106-17 72
Fig. 38 J-R Curve from Power Law Approach for Specimen A508-33 73
Fig. 39 J-R Curve from Power Law Approach for Specimen A508-24 74
Fig. 40 J-R Curve from Power Law Approach for Specimen A508-25 75
Fig. 41 J-R Curve from Power Law Approach for Specimen A508-19 76
Fig. 42 J-R Curve from Power Law Approach for Specimen A508- 6 77
Fig. 43 J-R Curve from Power Law Approach for Specimen A508- 1 78
Fig. 44 J-R Curve from Power Law Approach for Specimen A106-17 79
Fig. 45 J-R Curve from Power Law Approach for Specimen A106-18 80
Fig. 46 J-R Curve from Power Law Approach for Specimen A533-71 81
Fig. 47 J-R Curve from Power Law Approach for Specimen A533-76 82

Figures Page

Fig. 48 J-R Curve from Power Law Approach for Specimen HSLA-34 83

Fig. 49 J-R Curve from Power Law Approach for Specimen HSLA-35 84

Fig. 50 J-R Curve from Power Law Approach for Specimen HSLA-36 85

Fig. 51 J-R Curve from Power Law Approach for Specimen HY80-10 86

Fig. 52 J-R Curve from Power Law Approach for Specimen HY80-11 87

Fig. 53 J-R Curve from Power Law Approach for Specimen HY80-12 88

Fig. 54 Normalized Deformation Curves for A508 Steel Specimens Showing They Have Almost same Behaviors at the Beginning Region 89

LIST OF SYMBOLS

a, Δa	crack length and crack extension
a_e	Irwin's effective crack length modified to account for strain hardening
a_0, a_f	initial and final crack length
A_{pl}	plastic component of the area under the load versus displacement record
b	remaining uncracked ligament of the test specimen
B	thickness of a specimen
B_e	effective thickness of a side grooved specimen
B_N	net thickness of a side grooved specimen
C	elastic compliance
E	Young's modulus
$f(a/W)$	geometrical factor function used in K calibration
$g(b/W)$	function of normalized remaining uncracked ligament used for separable multiplicative functions of P
$G(a/W)$	function of normalized crack length used for separable mutiplicative functions of P
$H(v_{pl}/w)$	function of normalized plastic displacement used for separable multiplicative functions of P
J	potential energy release rate per unit crack length extension for ductile fracture
J_{el}, J_{pl}	elastic and plastic component of J
K	crack tip stress intensity factor
L, M, N	fitting constants in LMN function

α, n	material strain hardening constants used in the Ramberg-Osgood description
P	load
P_N	normalized load
P_0	limited load per unit thickness based on the yield stress
S	distance between three-point loaded bend specimen supports
T_i	components of traction vector
u_i	components of displacement vector
v	load-line displacement
v_{el}, v_{pl}	elastic and plastic component of v
w	strain energy density
W	specimen width
β, n, μ, κ	fitting constants in Eq. (3.11) and Eq. (3.12)
ε_{ys}	yield strain
ε_0	effective yield strain
ν	Poisson's ratio
σ_y	effective yield strength
σ_{ys}	yield strength
σ_{UTS}	ultimate (tensile) strength

1. INTRODUCTION

Since it was introduced by Rice[1], in 1968, the J-integral method of analysis has been viewed as a direct extension of linear elastic fracture mechanics (LEFM), into the elastic-plastic regime, and its physical and analytical basis are as powerful as LEFM. Its role was examined and its significance and application are shown as follows.

(1). The value of J is the numerical result of a line integral from the lower to the upper surface of a crack, independent of the particular path of integration [1]. i.e.

$$J = \int_{\Gamma} \left(w\, dy - T_i \frac{\partial u_i}{\partial x} ds \right) \tag{1.1}$$

(2). J is the strength of the crack tip elastic-plastic stress-strain field singularity, thus it may be regarded as the characteristic parameter [2,3].

(3). J can be seen as the potential energy release rate per unit crack extension for the non-linear elastic counterpart of an elastic-plastic material [4]. That is

$$J = -\frac{dU}{Bda} = -\int_0^v \frac{\partial P}{\partial a}\Big|_v dv = \int_0^P \frac{\partial v}{\partial a}\Big|_P dP \tag{1.2}$$

(4). J can be used as a fracture initiation criterion, defined as J_{Ic}, by reasoning that for a given material equal J values mean equal intensities of geometrically identical surrounding crack tip stress-strain fields. Thus, crack growth begins when a critical value of the strength of the field is attained [5,6].

(5). J can be used for constructing the material property J-R curve, as an extension of the G-R curve of LEFM. It applies even for significant amounts of crack growth under certain restrictions [7,8,9]. The J-R curve can also be used to analyze conditions for ductile instability [10,11].

As the essential fracture toughness property and criterion for materials which fail in a ductile manner, the J-R curve and J_{Ic} value can be measured using two standard ASTM test methods, E813 and E1152 [12,13]. According to these standard methods, to develop J_{Ic} values and J-R curves triplets of information are needed: load displacement and crack length. They are obtained from tests of fatigue precracked fracture toughness specimens. Traditionally, J_{Ic} values from E813 have been developed using two techniques [12]. The first, called the multiple specimen method, uses a series of specimens tested to different crack opening displacements, each developing a single point of J versus crack extension. The second, called single specimen method, uses instrumentation to develop values of J versus crack extension from one specimen. The single specimen method can also be used to develop the full J-R curves in accordance with ASTM 1152.

Obviously, the single specimen technique has advantages. It develops more information, namely the full J-R curve, requires fewer specimens and gives a more satisfactory result.

In general, to develop J-R curves from the single specimen method, the load and displacement can be measured directly on the test specimen while the crack extension measurement can be only obtained by using an indirect measurement, such as the elastic unloading compliance method or the electrical potential drop method. This requires sophisticated equipment and advanced testing techniques, which may be sometimes a problem to some laboratories. In some special cases, such as hot cell testing of irradiated materials, experimental measuring the displacement may even be difficult and only the measurements of load, crack extension and final plastic displacement can be obtained from the testing. To develop J-R curves in such a case may present some difficulty.

Recently Dr. Landes and his group have introduced a new method, labeled normalization, to develop the full J-R curve from load versus displacement records with no crack extension monitoring equipment [14,15,16,17]. This method was based on the " key curve " approach introduced by Joyce [18]. Using the normalized plastic deformation curve (i.e. key curve) assumption , the load, displacement and crack length can be functionally related. If a suitable functional form is assumed, the individual normalized plastic deformation curve can be determined uniquely for each specimen . Once known, it can be used to determine crack length directly from a single specimen test record. This method gives all the information needed to develop both the J_{Ic} value of E813 and the J-R curve of E1152.

Several versions of this method have been proposed. The first one used a power law with two unknown fitting parameters as the functional form [14,15]. The two unknown fitting parameters could be determined from the test details at the original and final crack length. This functional form worked satisfactorily for the materials which did not have extensive plastic deformation ($v_{pl}/W < 0.05$) during the fracture process. The second version used a combination of power law plus straight line as the assumed functional form [16]. This is based on the fact that the normalized plastic deformation curve appears to have a straight line character for materials with extensive plastic deformation ($v_{pl}/W > 0.05$). The power law plus straight line functional form gave better results than the pure power law method because it more generally described the deformation character observed in a test specimen. However, this functional form was awkward to deal with, it needed a point of transition from power law to straight line. This point had to be chosen and fitting constants determined from points where crack length was not known. The third version used the so-called LMN function as the functional form assumed to relate normalized load and plastic displacement [17]. It was taken from the work of Orange [19] and has the general form

$$H(v_{pl}/W) = \frac{[\, L + M\,(v_{pl}/W)\,]\,(v_{pl}/W)}{N + (v_{pl}/W)} \tag{1.3}$$

where $H(v_{pl}/W)$ is a plastic deformation function and L, M and N are fitting constants. This function has the character of resembling a power law for small v_{pl}/W (when $v_{pl}/W << N$) and a straight line for large v_{pl}/W (when $v_{pl}/W >> N$). The transition between the two behaviors is smooth. Therefore, it makes the normalization method more generally applicable to ductile materials. The normalization method with this function form, called LMN normalization method, was applied to more than 60 specimens made from 6 different metallic materials to develop J-R curves from load versus displacement records [17]. It worked extremely well and the results remarkably improved compared to those from the earlier two functional forms.

The objective of this paper is to try to use LMN normalization method to develop J-R curves from load versus crack length records where displacement has not been measured. This could make it possible for the single specimen technique to be used in some special cases, such as high temperature or hot cell testing, where a displacement measurement may be difficult. It is based on the idea that the LMN function uniquely relates the load, plastic displacement and crack length and once it is determined, it can be used with the compliance calibration function to determine any one of the three parameters provided the other two are known. The first step of this work will give some background on the new method, including the method of developing J-R curves from the ASTM ductile fracture test standard using the elastic unloading compliance method and the LMN normalization method. Then based on these, the LMN normalization method will be used to demonstrate how to develop J-R curves from load versus crack length records. The first step in this is to demonstrate how to determine the LMN function from the load versus crack length record. Three approaches will be introduced for determining the LMN function. Finally these approaches will be applied to more than 20 specimens, which have an order of magnitude difference in size (from 1/2T to 10T) and are made from 5 different metallic materials, to demonstrate how to develop the J-R curves. The results will be compared with those analyzed previously by elastic compliance method and by LMN normalization method applied to load versus displacement records.

2. BACKGROUND ON THE NEW APPROACHES

The new approaches for developing J-R curves from load versus crack length records will be derived based on the ASTM ductile fracture standard test methods, E813 and E1152, and the LMN normalization method. Before introducing the new approaches, some background on the standard methods and the LMN normalization method will be given.

2.1 The ASTM Standard Test Methods, E813 and E1152, for Developing J_{Ic} Values and J-R Curves

As an alternate to the line integral definition, an equally valid definition provided by Rice [4], for J is in the form of potential energy release rate per unit crack area, given by

$$J = -\frac{dU}{Bda} = -\int_0^v \frac{\partial P}{\partial a}\Big|_v \, dv = \int_0^P \frac{\partial v}{\partial a}\Big|_P \, dP \qquad (1.2)$$

This form was used by Begley and Landes to do the first experimental evaluation of J where they obtained J as a function of crack length and level of applied deformation(v or P) for different geometrical configurations in 1972 [5,19]. After their critical experiments, many significant works on evaluating J and J-R curves were done by Bucci et al. [20], Rice et al. [21], Landes and Begley [7], Clarke et al. [22], McCabe and Heyer [8,9], Ernst et al. [23], Hudak and Saxena [24] and others [25]. Based on these works, two standard ductile fracture test methods, E813 and E1152, have been developed and issued by ASTM for evaluating J_{Ic} values and J-R curves [12,13].

For developing J_{Ic} values and J-R curves by using ASTM standard test method the standard compact specimen (CT) is used. This is pin-loaded in tension and has an initial normalized crack length (a_0/W) of 0.5 to 0.7. An alternate specimen is the three-point loaded bend specimen (SENB), which is a single edge-cracked beam and also has an initial normalized crack length(a_0/W) of 0.5 to 0.7. To conduct the test, the single specimen method is preferred. The measurements of applied load, P, load-line displacement, v, and crack length, a, must be obtained from the test. In general, load versus load-line displacement can be recorded directly either digitally for processing by a computer or autographically with an "x-y" plotter via the load transducer and displacement gage. Crack length , on the other hand, cannot usually be measured directly. For the single specimen test method, crack length can be measured by using the elastic compliance method or DC potential drop method. The elastic compliance method uses the elastic compliance measurements to determine crack length and crack extension. These measurements are taken on a series of unloading/reloading segments spaced along the load versus displacement record [22,26]. The crack length measurements then can be obtained from the elastic compliance measurements. For CT specimen, they are given by [24]

$$a_i/W = 1.00196 - 4.06319u_{LL} + 11.242u_{LL}^2 - 106.043u_{LL}^3 + 464.335u_{LL}^4 - 650.677u_{LL}^5 \tag{2.1}$$

where

$$u_{LL} = \frac{1}{(B_eEC)^{1/2} + 1}$$

E is the modulus of elasticity

B_e is the effective thickness and $B_e = B - (B - B_N)^2 / B$

C_i is the specimen elastic compliance on an unloading/reloading sequence and $C_i = \Delta v_i / \Delta P_i$

For the SENB specimen they are given by [28]

$$a_i/W = 0.999748 - 3.9504\ U_x + 2.9821\ U_x^2 - 3.21408\ U_x^3$$
$$+ 51.51564\ U_x^4 - 113.031\ U_x^5 \qquad (2.2)$$

where

$$U_x = \frac{1}{(4B_eWEC_i/S)^{1/2} + 1}$$

C_i is the specimen elastic compliance on an unloading/reloading sequence and $C_i = \Delta v_x / \Delta P_i$

Δv_x is the increment to crack mouth opening displacement

S is the distance between specimen supports.

The DC potential drop method uses the changes in the electrical resistance of a specimen to determine crack extension. It has become more popular as the electronic equipment used has improved. After many years of development, these two method are now used routinely and with very good success in many laboratories. However, they do require sophisticated equipment and advanced testing techniques to make them work successfully.

Once the measurements of applied load, load-line displacement and crack length are obtained, the J value can be evaluated at any point by using the method provided by Ernst et al. [23]. That is

$$J = J_{el} + J_{pl} \tag{2.3}$$

were

J_{el} is the elastic component of J

J_{pl} is the plastic component of J

and

$$J_{pl(i)} = [\, J_{pl(i-1)} + (\frac{\eta_i}{b_i}) \frac{A_{pl(i)} - A_{pl(i-1)}}{B_N}] \, [\, 1 - (\gamma_i) \frac{a_i - a_{(i-1)}}{b_i}] \tag{2.4}$$

where

b_i is the remaining uncracked ligament and $b_i = W - a_i$

for CT specimen

$\eta_i = 2.0 + 0.522\ b_i/W$

$\gamma_i = 1.0 + 0.76\ b_i/W$

for SENB specimen

$\eta_i = 2.0$

$\gamma_i = 1.0$

$[\, A_{pl(i)} - A_{pl(i-1)} \,]$ is the increment of plastic area under the load versus load-line displacement record between lines of constant displacement at points (i - 1) and (i), and

$$A_{pl(i)} = A_{pl(i-1)} + \frac{[P_{(i)} + P_{(i-1)}]\ [v_{pl(i)} - v_{pl(i-1)}]}{2} \tag{2.5}$$

where

$v_{pl(i)}$ is the plastic part of the load-line displacement and

$$v_{pl(i)} = v_{(i)} - v_{el(i)} = v_{(i)} - P_i C_i$$

C_i is the compliance ($\Delta v_i/\Delta p_i$) required to give the current crack length, a_i. Also for the tests that do not utilize the elastic compliance technique, C_i can be determined from the knowledge of a_i/W using the following equations [24], for the CT specimen

$$C_i = \frac{1}{EB_e}\left(\frac{W + a_i}{W - a_i}\right)^2 [\ 2.1630 + 12.219(a_i/W) - 20.065(a_i/W)^2$$

$$- 0.9925(a_i/W)^3 + 20.609\ (a_i/W)^4 - 9.9314(a_i/W)^5\ ] \qquad (2.6)$$

for the SENB specimen

$$C_i = \frac{1}{EB_e}\left(\frac{S}{W - a_i}\right)^2 [\ 1.193 - 1.980(a_i/W) + 4.478(a_i/W)^2$$

$$- 4.443(a_i/W)^3 + 1.739(a_i/W)^4] \qquad (2.7)$$

and the J_{el} can be given by

$$J_{el} = \frac{(K_i)^2\,(1 - \nu^2)}{E} \qquad (2.8)$$

where

ν is the Poisson ratio

K_i is the crack tip stress intensity factor and K_i can be determined from ASTM standard test method E399. That is

for the CT specimen:

$$K_i = \frac{P_i}{(BB_NW)^{1/2}} f(a_i/W) \qquad (2.9)$$

With

$$f(a_i/W) = \frac{(2 + a_i/W)}{(1 - a_i/W)^{3/2}} [\ 0.886 + 4.64(a_i/W) - 13.32(a_i/W)^2$$

$$+14.72(a_i/W)^3 - 5.6(a_i/W)^4\ ] \qquad (2.10)$$

for the SENB specimen

$$K_i = \frac{P_i \ S}{(BB_N)^{1/2} W^{3/2}} \ f(a_i/W) \tag{2.11}$$

with

$$f(a_i/W) = \frac{3 \ (a_i/W)^{1/2}}{2(1 + 2a_i/W)} (1 - a_i/W)^{3/2} \ \{ \ 1.99 - (a_i/W) \ (1-a_i/W)$$
$$[\ 2.15 - 3.93(a_i/W) + 2.7(a_i/W)^2 \ ] \ \} \tag{2.12}$$

Also , the crack extension can be given by

$$\Delta a_i = a_i - a_0 \tag{2.13}$$

where a_0 is the initial crack length.

At this point, the J-R curve can be plotted from the J-integral values and the corresponding crack extension values, provided the validity requirements of ASTM standard test method, E1152, are satisfied. A typical J-R curve from compliance method is given in Fig. 1. From this the J_{Ic} values can be determined by using at least four qualifying data points which lie within the two specified exclusion lines. These data reflect the material resistance to crack growth. The J versus crack growth behavior is approximated with a best-fit power law relationship. A blunting line is drawn, approximating crack tip stretch effects. The blunting line is calculated from material flow properties, using the expression

$$J = 2\sigma_y \Delta a \tag{2.14}$$

where σ_y is the effective yield strength and $\sigma_y = (\sigma_{ys} + \sigma_{UTS}) / 2$.

An offset line parallel to the blunting line but offset by 0.2 mm (0.008 in) is drawn. The intersection of this line and the power law fit defines J_{Ic}, provided the validity requirement of ASTM standard test method, E813, are satisfied.

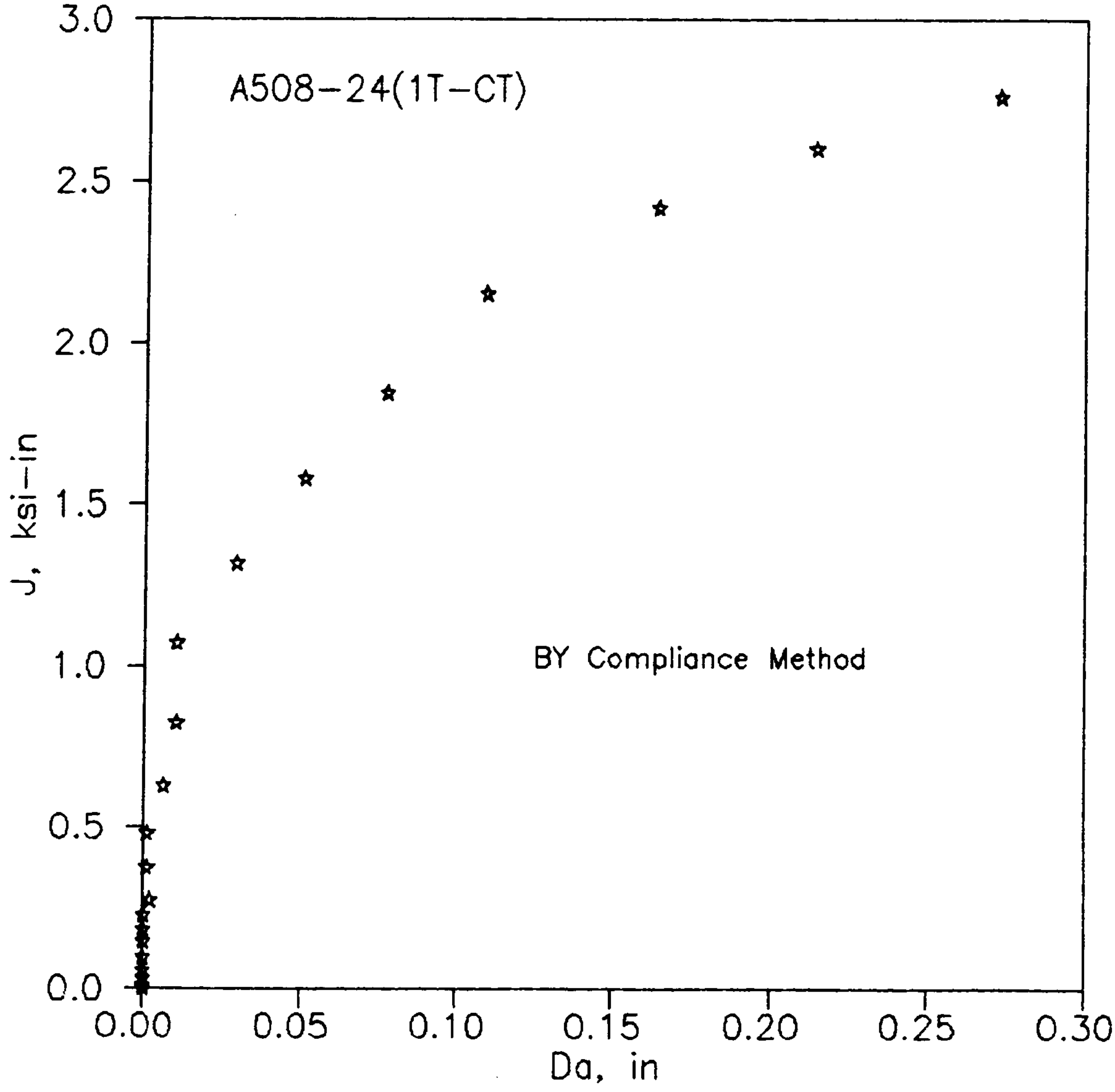

Fig. 1 A Typical J-R Curve from Elastic Compliance Method

2.2 The LMN Normalization Method

The idea of using flow properties of material to determine crack length for developing J-R curves directly from load versus displacement records was first suggested by Ernst et al. [28,29] and later given the label "key curve" method [18]. In this work, a universal normalized plastic deformation curve (i.e. key curve) was assumed to exist for a given material. Once it was measured, it would apply to similar specimens of the same material. Although the technical basis of the method is sound, it never was widely used because some of the details needed for applying the method had never been satisfactorily developed until Landes et al. recently proposed their method of normalization.

The method of normalization introduced by Landes et al. [15,16,17] was derived from the key curve analysis. Rather than assuming a universal normalized plastic deformation curve exists for a material, they used the individual normalized plastic deformation curve for each specimen. If a suitable functional form of the normalized plastic deformation curve was assumed, the normalized plastic deformation curve can be determined from the detail of the load versus displacement record for each specimen. Then the normalized plastic deformation curve related the load, displacement and crack length uniquely and can be used to determine the crack length for developing J-R curve.

To use the method of normalization it was assumed that during a test of a precracked specimen, the load, displacement and crack length can change continuously. Since these are the only interacting variables during the test, they must be related by an arbitrary function F:

$$P = F\ (a/W,\ v/W) \tag{2.15}$$

where crack length, a, and displacement, v, are nondimensionalized by the specimen width, W. An important development in the analysis of load, displacement and crack length relationship was made by Ernst [28,29], who showed that the load P can be represented by separable multiplicative functions of the normalized crack length (a/W) and the normalized plastic displacement (v_{pl}/W) when displacement is divided into elastic and plastic components

$$v = v_{el} + v_{pl} \tag{2.16}$$

and

$$P = G\ (a/W)\ H\ (v_{pl}/W) \tag{2.17}$$

In fact, the load P, elastic displacement v_{el} and crack length a are related by

$$v_{el} = P\ C(a/W) \tag{2.18}$$

where C(a/W) is the compliance function and can be determined by Eq. (2.6) or (2.7) for compact specimen and three-point bend specimen respectively. If both of G(a/W) function and $H(v_{pl}/W)$ function are known, the load displacement and crack length have an unique relationship.

The function G(a/W) is dependent on the particular specimen geometry and can be determined for a specimen type if the J calibration is known; this was demonstrated by Ernst et al. [23] and Sharobeam and Landes [30,31], where the plastic eta function, η_{pl}, was used to determine G(a/W)

$$\eta_{pl} = -\left(\frac{b}{W}\right)\left[\frac{G'(a/W)}{G(a/W)}\right] \tag{2.19}$$

where

b is the remaining uncracked ligament and $b = W - a$

For the bend-type specimen, G(a/W) can be written in terms of b in the form

$$P = \frac{Bb^2}{W}\, g(b/W)\; H(v_{pl}/W) \tag{2.20}$$

and

$$\eta_{pl} = \left[\, 2 + \frac{b}{W}\, \frac{g'(b/W)}{g(b/W)}\right] \tag{2.21}$$

It has been suggested [23] that for the compact specimen

$$\eta_{pl} = 2 + 0.522\left(\frac{b}{W}\right) \tag{2.22}$$

the function g(b/W) is then automatically implied by Eq.(2.21) combined with Eq.(2.22)

$$g(b/W) = e^{0.522b/W} \tag{2.23}$$

for three-point bend specimen (with span/width radio = 4)

$$\eta_{pl} = 2 \tag{2.24}$$

with

$$g(b/W) = 1 \tag{2.25}$$

The deformation function $H(v_{pl}/W)$ is material dependent and varies from one material to another. It depends on flow strength, hardening character and other material features and can be evaluated most generally in a graphical format by separating Eq.(2.20) into its crack length dependent form, defined as P_N, that is

$$P_N = \frac{P\;W}{Bb^2 g(b/W)} = H(v_{pl}/W) \tag{2.26}$$

Plotting P_N versus (v_{pl}/W) defines graphically the functional form of $H(v_{pl}/W)$; this is shown schematically in Fig. 2. The curve of P_N versus (v_{pl}/W), called the normalized plastic deformation curve, contains all the information relating P, v_{pl} and a. Therefore, given any two of the three parameters, the third can be determined, provided the normalized deformation function is known. This principle forms the basis of the method of normalization. The basic idea of normalization suggested that a functional form could be assumed that was general for metals. This functional form would have unknown constants that could be determined from details of the test.

The early normalization analyses [15,16] used a function $H(v_{pl}/W)$ which appeared to have a power law character when $(v_{pl}/W) < 0.05$ and a straight line character when $(v_{pl}/W) > 0.1$. The latest suggestion for $H(v_{pl}/W)$ function form was LMN function which was adopted from the work of Orange [27]. The general form of LMN function has been introduced in section 1, that is

$$H(v_{pl}/W) = \frac{[\, L + M(v_{pl}/W) \,]\,(v_{pl}/W)}{N + (v_{pl}/W)} \tag{1.3}$$

where L, M, N are fitting constants. This function has the character of a power law when $(v_{pl}/W) \ll N$ and a straight line when $(v_{pl}/W) \gg N$. The transition between the two behaviors is smooth. This agrees very well with those of the function $H(v_{pl}/W)$ observed from the early work of the normalization analysis. So it seems to be a very suitable selection for the functional form of $H(v_{pl}/W)$.

The LMN function has three constants and therefore also needs three calibration points to determine them. The LMN normalization

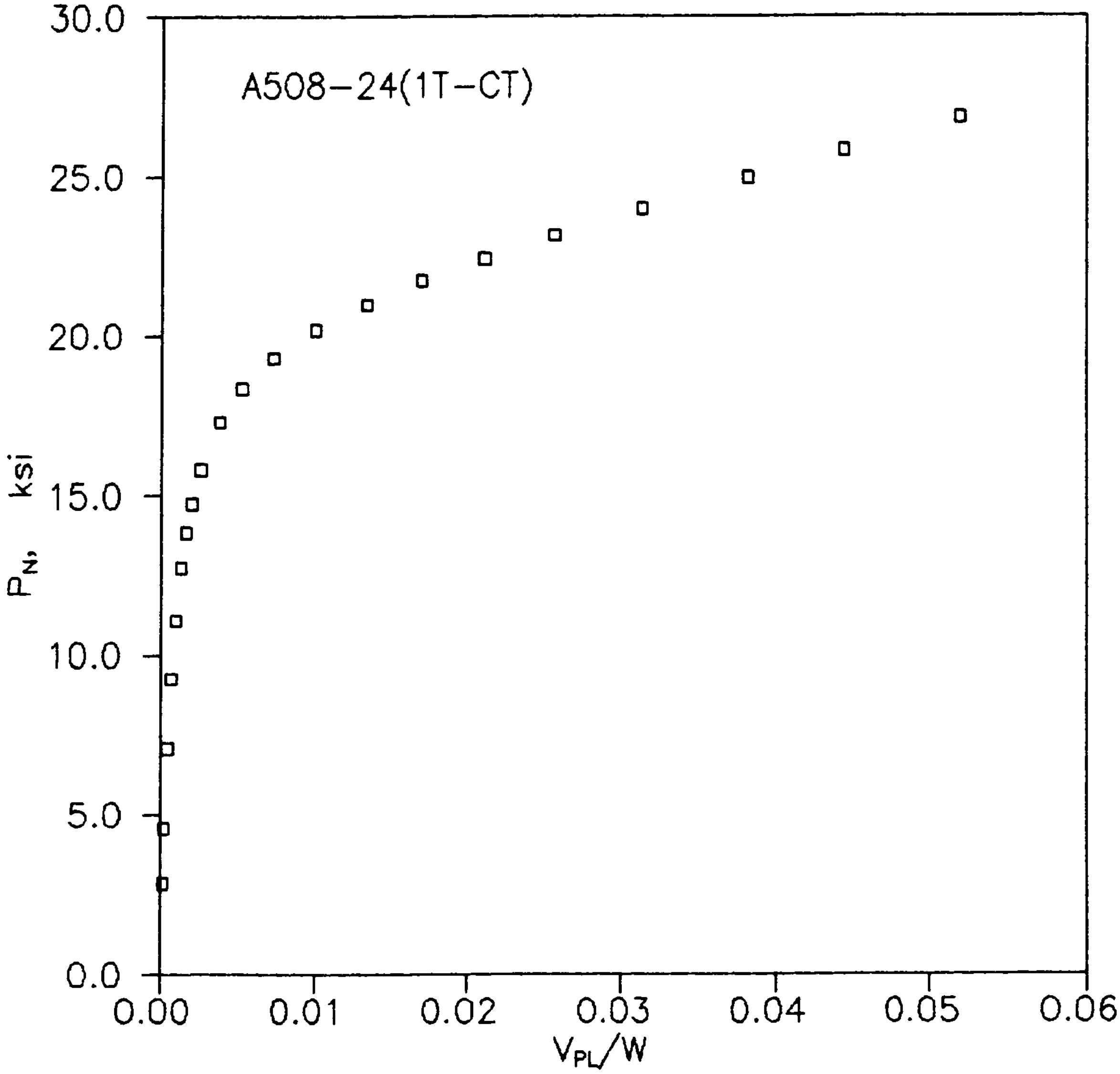

Fig. 2 Schematic of Normalized Load Versus Plastic Displacement Curve

method provided by Landes et al. [17, 33] used an enforced blunting, which gives several calibration points at the beginning of the plastic deformation curve, an intermediate calibration point and a final calibration point measured at the final value of crack length to determine the LMN function. This idea was illustrated schematically in Fig. 3.

The idea of using enforced blunting to get several beginning calibration points was based on the fact that the blunting behavior was observed in the results from other multiple specimen or single specimen techniques. This should be reproduced when the normalized deformation function is used. The LMN normalization method used the ASTM E813 blunting equation

$$\Delta a = J / 2\sigma_y \tag{2.27}$$

combined with Eq.(2.3) through Eq.(2.13) and Eq(2.26) to obtain these beginning calibration points.

The second part of the construction of the deformation function requires an intermediate calibration point which cannot be determined for a known crack length. The idea for this point came from a careful study of the normalized deformation behavior of many different steel specimens. It was observed that by dividing the normalized load, P_N, by flow stress, σ_y, and dividing (v_{pl}/W) by $\alpha\varepsilon_0$, where α is a material constant used in a power law hardening stress-strain description and ε_0 is σ_y/E, where E is the elastic modulus, gives a fairly consistent normalized deformation curve for all materials. This is illustrated in Fig. 4. In particular there is a point near the transition between the power law region and straight line

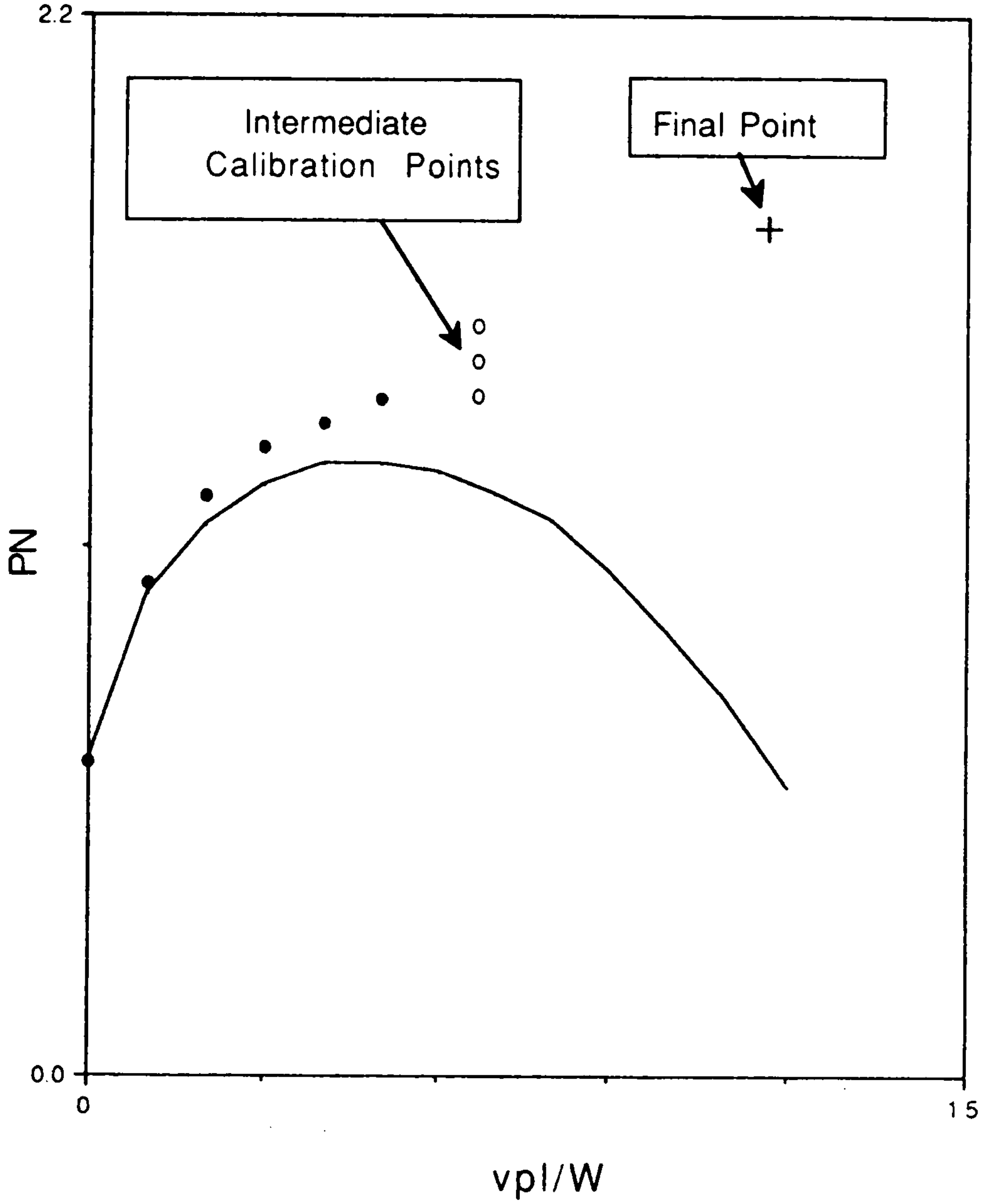

Fig. 3 Schematic of Calibration Points for LMN Function Fit

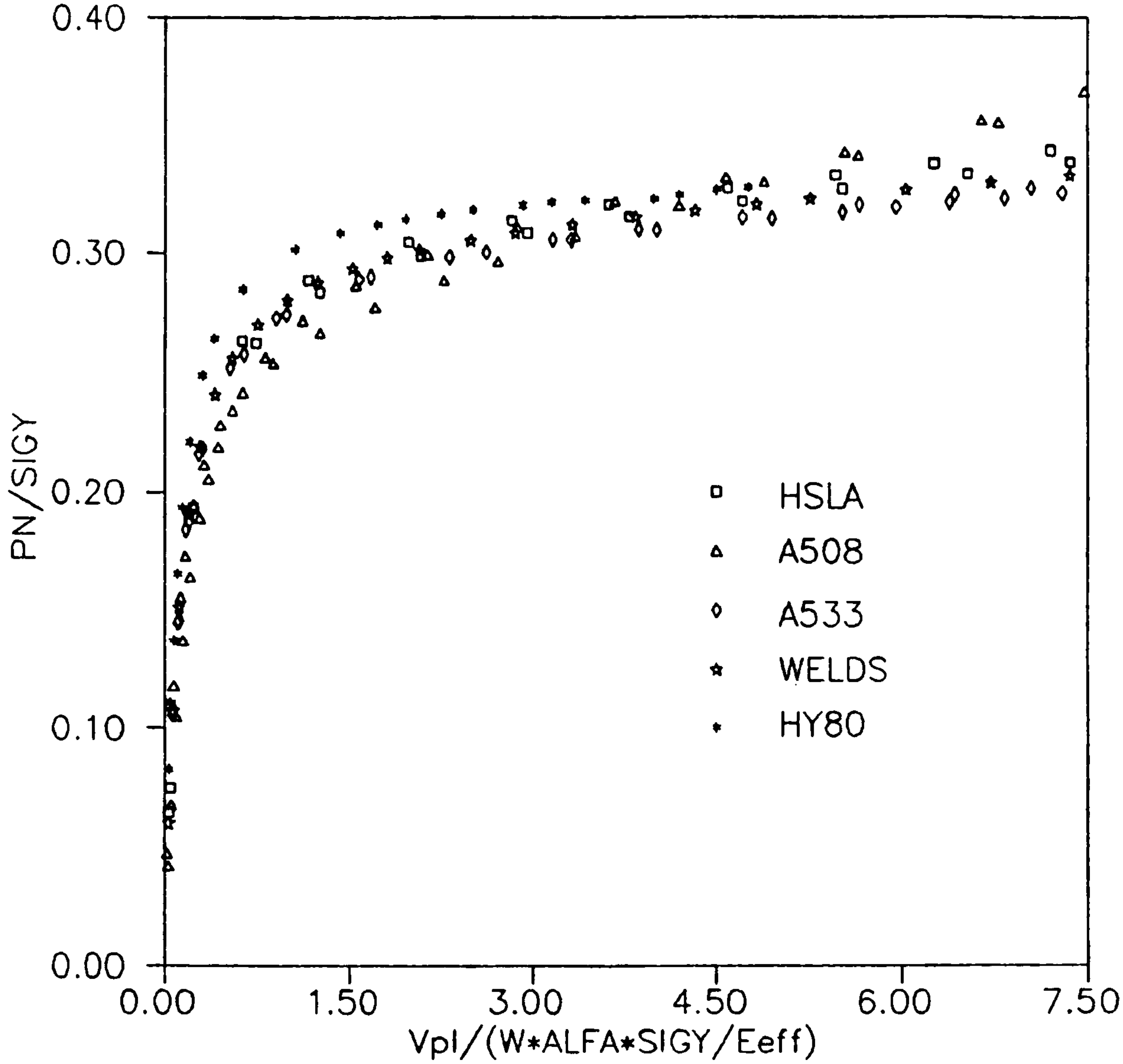

Fig. 4 Normalized Load Versus Plastic Displacement Showing Fixed Intermediate Calibration point

behavior where all of curves appeared to converge [32]. This was a point of approximately $P_N = 0.32\ \sigma_y$ and $v_{pl}/W = 4.5\ \alpha\varepsilon_0$. This was first adapted as a fixed point. However in using this point, slight material variations caused scatter in results, because it was in a sensitive region for J-R curve analysis. The LMN normalization method then picked this as an intermediate calibration point which can vary slightly in a range of P_N values but was fixed at $v_{pl}/W=4.5\alpha\varepsilon_0$. It was first picked below the correct value of P_N and then varied while the LMN function were determined.

The final calibration point was obtained from the test record and the final crack length which was measured from the surface of the broken specimen.

The fitting of the LMN function then proceeded using the three types of calibration points described, each one of the beginning calibration points from the enforced blunting with the variable intermediate calibration point and the final calibration point formed a set of calibration points. The variable intermediate point was varied and fits were made for every set of calibration points and several sets of fitting constants L, M, N were obtained each time. The selection of the intermediate point was the one that gave the minimum fitting deviation for all the sets of fitting constants L, M, N. The values of constants L, M, N for specifying the LMN function then can be taken from the averages of fitting values respectively from the set that gave minimum fitting deviation.

The LMN function uniquely relates the load, the plastic displacement and the crack length. Once it is determined, it can be used to determine crack length from the load versus displacement record. That is, the combination of Eq.(1.3) and Eq. (2.6) gives

$$P_N = \frac{P\ W}{Bb^2 g(b/W)} = \frac{[\ L + M\ (v_{pl}/W)\ ]\ (v_{pl}/W)}{N + (v_{pl}/W)} \qquad (2.27)$$

where

$b = W - a$

$v_{pl} = v - v_{el}$

$v_{el} = P\ C(a/W)$

and C(a/W), g(b/W) were given in Eq.(2.6) or (2.7) and Eq.(2.23) or (2.25)

The unknown crack length, a, is embedded in Eq (2.27) and (2.6) or (2.7) with Eq. (2.16), (2.18) and can best be solved iteratively by using a computer.

Once the crack length values were determined, the J-R curve can be developed from the measurements of crack length with the load versus displacement record. This can be achieved either by integrating the deformation function directly or by using the E1152 Eq.(2.3) through Eq.(2.13).

The LMN normalization method has been applied to a number of specimens made from 6 different metallic materials to develop J-R curves and J_{Ic} values. As previously mentioned the results were excellent [17].

3. DEVELOPING J-R CURVES FROM LOAD VERSUS CRACK LENGTH RECORDS

3.1 Introduction

In some special cases, such as the high temperature testing or the hot cell testing of irradiated materials, it may be difficulty to get a displacement measurement. For these cases only load versus crack length records can be measured during the test. Also the final plastic displacement can be obtained after the test from the permanent set of the specimen. The ASTM standard test methods, E813 and E1152, cannot be used for analyzing J-R curves and J_{1c} values in such a condition. A new method must be developed.

The LMN normalization method introduced by Landes et al.[15,16,17] has been successfully used to develop J-R curves from load versus displacement records without crack length measurements. In this method the normalized load versus plastic displacement, expressed by the LMN function, relates the load, plastic displacement and crack length uniquely. Once it is determined, it can be used to predict any one of the three parameters provided the other two are known. Therefore, the LMN normalization method could be used to predict the plastic displacement and then to develop J-R curve from load versus crack length record.

To construct the LMN function

$$P_N = \frac{P\ W}{Bb^2 g(b/W)} = \frac{[\ L + M(v_{pl}/W)\ ]\ (v_{pl}/W)}{N + (v_{pl}/W)} \qquad (2.27)$$

from the load versus crack length record, the normalization load P_N can be evaluated from the test record directly. For determining the LMN function three calibration points are needed. The final calibration point can be obtained at the end of the test by determining the final physical plastic displacement. The intermediate calibration point can be determined in the process of fitting the LMN function by varying the variable intermediate point in values of P_N at constant $v_{pl}/W = 4.5\alpha\varepsilon_0$ provided several beginning calibration points are known. Therefore, the key determining the LMN function for developing the J-R curve from the load versus crack length record is in determining how to obtain several beginning calibration points. This study tries to use some approximate techniques which incorporate material flow properties to predict these points. Three approaches are proposed here for determining these beginning calibration points.

3.2 Using the "Handbook" Method to Obtain the Beginning Calibration Points

An engineering approach provided by Kumar et al.[34] for calculating J and plastic load-line displacement had been introduced in the GE-EPRI Elastic-Plastic Fracture Analysis Handbook. The J and plastic displacement equations are given as

$$J = J_{el} + J_{pl}$$

$$J_{el} = \frac{K^2(a_e)}{E'} \tag{3.1}$$

with

$$K(a_e) = \frac{P}{(BB_NW)^{1/2}} f\left(\frac{a_e}{W}\right)$$

and

$$J_{pl} = \alpha\sigma_{ys}\varepsilon_{ys} b h_1(a/W,\ n)(P/P_0)^{n+1} \tag{3.2}$$

$$v_{pl} = \alpha\varepsilon_{ys} a h_3(a/W,\ n)(P/P_0)^{n} \tag{3.3}$$

where

α and n are the material hardening constants used in the Ramberg-Osgood fit $\frac{\varepsilon}{\varepsilon_{ys}} = \frac{\sigma}{\sigma_{ys}} + \alpha\left(\frac{\sigma}{\sigma_{ys}}\right)^n$.

σ_{ys} is the yield stress.

ε_{ys} is the yield strain, and $\varepsilon_{ys} = \sigma_{ys} / E$

a_e is the Irwin's effective crack length modified to account for strain hardening and

$$a_e = a + \phi\, r_y$$

with

$$r_y = \frac{1}{\beta\pi}\left(\frac{n-1}{n+1}\right)\left(\frac{K}{\sigma_0}\right)^2 \tag{3.4}$$

and

$$\phi = \frac{1}{(P/P_0)^2} \tag{3.5}$$

where

$\beta = 2$ for plane stress

$\beta = 6$ for plane strain

P_0 is the limited load per unit thickness based on the yield stress, for compact specimen it is given as

$$P_0 = 1.455\ \eta b \sigma_0 \qquad \text{for plane strain} \tag{3.6}$$

$$P_0 = 1.071\ \eta b \sigma_0 \qquad \text{for plane stress} \tag{3.7}$$

with $$\eta = [\ (2a/b)^2 + 2(2a/b) + 2\ ]^{1/2} - [2a/b + 1] \tag{3.8}$$

Also $h_1(a/W, n)$ and $h_3(a/W, n)$ are functions determined on a/W and n. Their values are tabulated in the EPRI Elastic-Plastic Handbook. $f(a_e/W)$ is a geometry factor given by Eq.(2.10) and Eq.(2.12) for the CT specimen and SENB specimen respectively.

$$E' = E \qquad \text{for plane stress}$$

$$E' = \frac{E}{1-\nu^2} \qquad \text{for plane strain}$$

Eq.(3.1) through (3.3) are valid for small effective crack extensions. These equations can be used to obtain the beginning calibration points from load versus crack length record. The value of plastic displacement, v_{pl}, can be evaluated by using Eq(3.3) directly, or in a indirect way, by using Eq(3.2) to evaluate J_{pl} first and then solving Eq.(2.4) and (2.5) by substituting J_{pl} into these equations to get v_{pl}. This engineering approach has been applied to several single specimen test records to evaluate the J values and plastic displacement for obtaining the beginning calibration points, these tests had previously been conducted and analyzed using the elastic compliance method. Because the hardening constants from the true stress-true strain were not available for these materials, the Bloom method [39] was used here to give the approximate hardening constants, α and n, of the materials used in these tests. The evaluations were conducted in the range of $P < P_{max}$ because only a few beginning calibration points are needed and the engineering approach can give better results for small crack extensions. Some examples of the beginning calibration points obtained from the Handbook approach are shown in Fig. 5 through Fig. 12 and compared with the results obtained from the elastic compliance method.

From these results it can be seen that the specimens from A508 steel gave more satisfactory results than those from A533 steel and HSLA steel. This may be caused by using the Bloom method to evaluate the hardening constants α and n, because the Bloom method can only roughly give an evaluation for the hardening constants α and n. If the hardening constants α and n are obtained from the true stress-true strain test record, the results may be expected to improve. Also it can be seen that for the same material each specimen gave different result agreement when compared with the corresponding result from the compliance method. The A508-24 (this means the specimen No. 24 made from A508 steel), A533-76 and HSLA-36 specimens gave better agreement than others made from same material respectively. This may be due to the engineering approach itself. It may be noted that this method is an engineering approximation. It is based on using the same material flow property to evaluate the J values and plastic displacements for all the specimens of the same material. But some materials tend to have the variability for different specimens and this approach is very sensitive when material flow properties vary. It should be pointed out that this engineering approach gave more accurate results for evaluating the J_{pl} values (using Eq.(3.2)) than for evaluating the

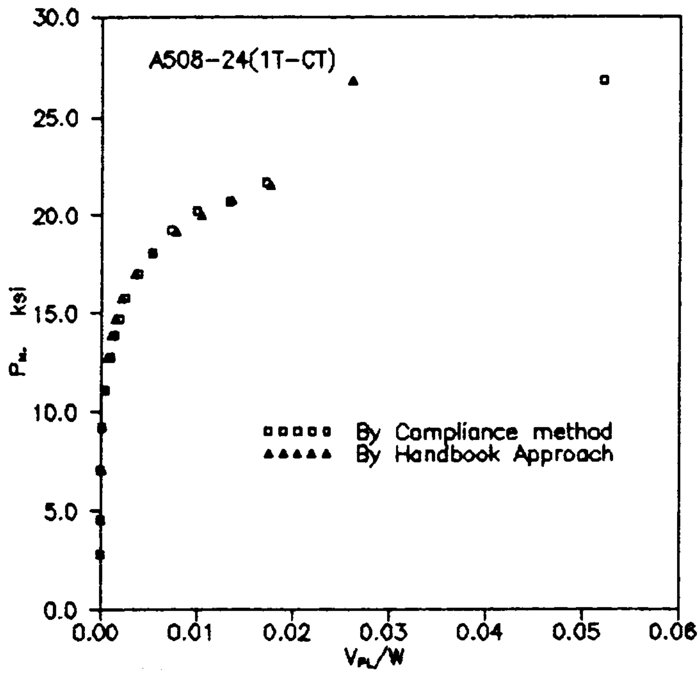

Fig. 5 The Beginning and Final Calibration Points Determined from the Handbook Approach for Specimen: A508-24

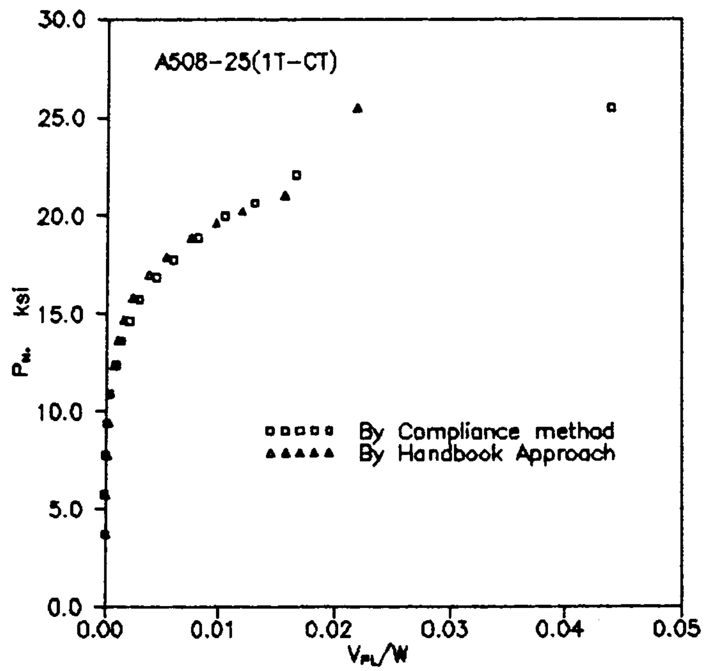

Fig. 6 The Beginning and Final Calibration Points Determined from the Handbook Approach for Specimen: A508-25

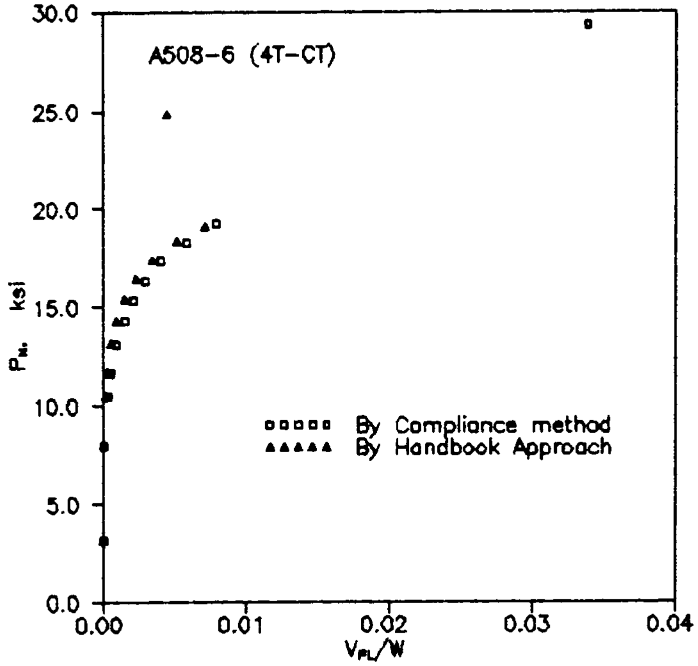

Fig. 7 The Beginning and Final Calibration Points Determined from the Handbook Approach for Specimen: A508-6

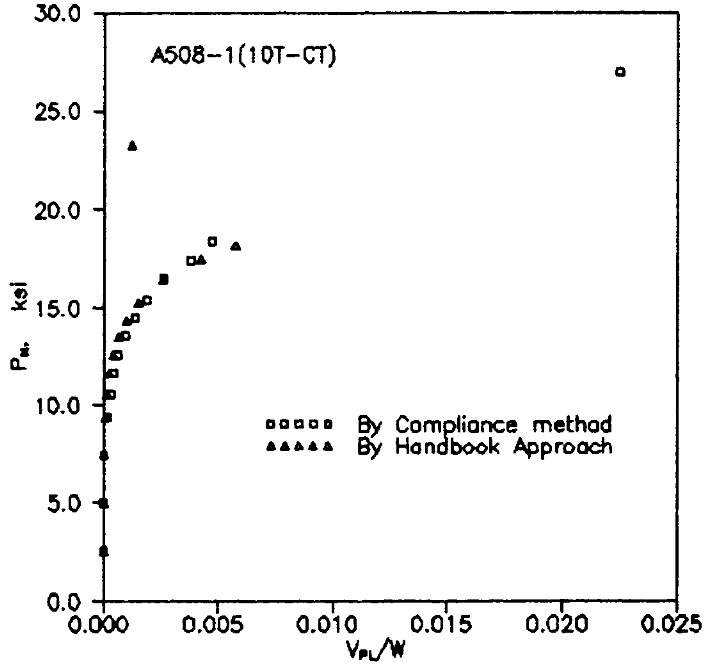

Fig. 8 The Beginning and Final Calibration Points Determined from the Handbook Approach for Specimen: A508-1

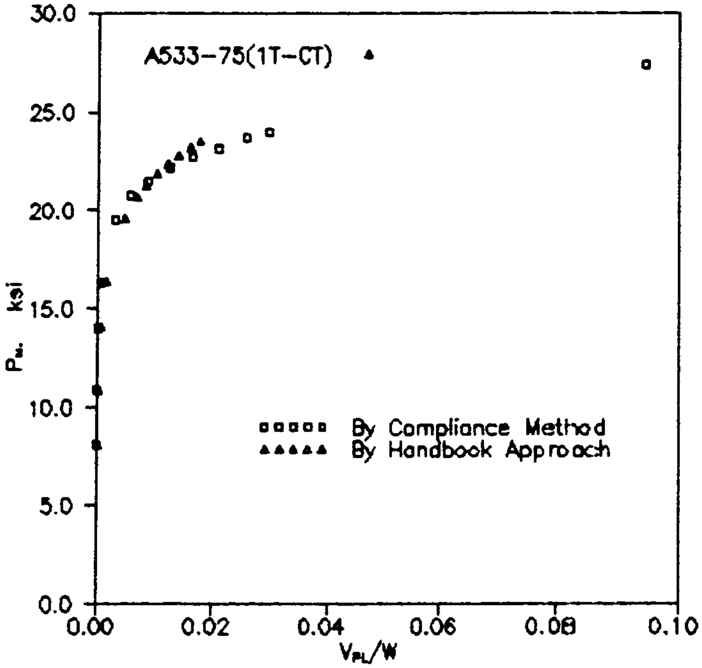

Fig. 9 The Beginning and Final Calibration Points Determined from the Handbook Approach for Specimen: A533-75

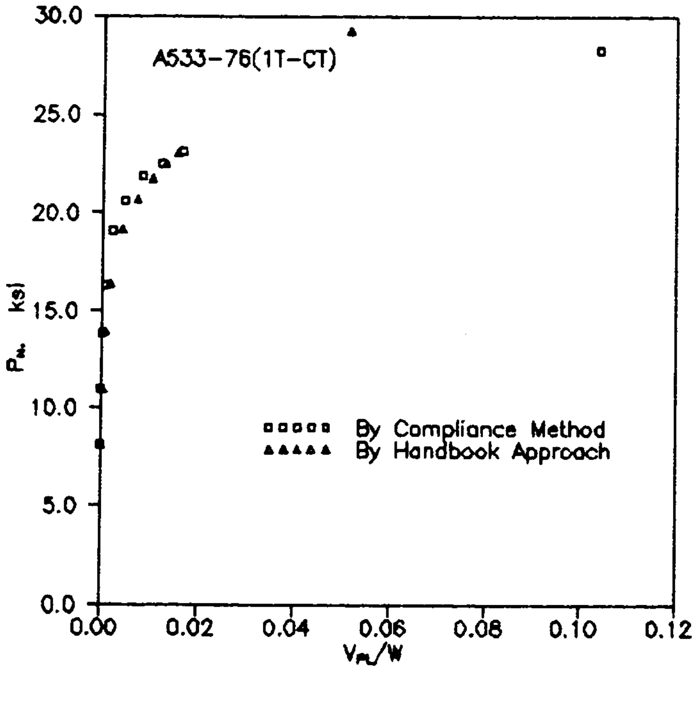

Fig. 10 The Beginning and Final Calibration Points Determined from the Handbook Approach for Specimen: A533-76

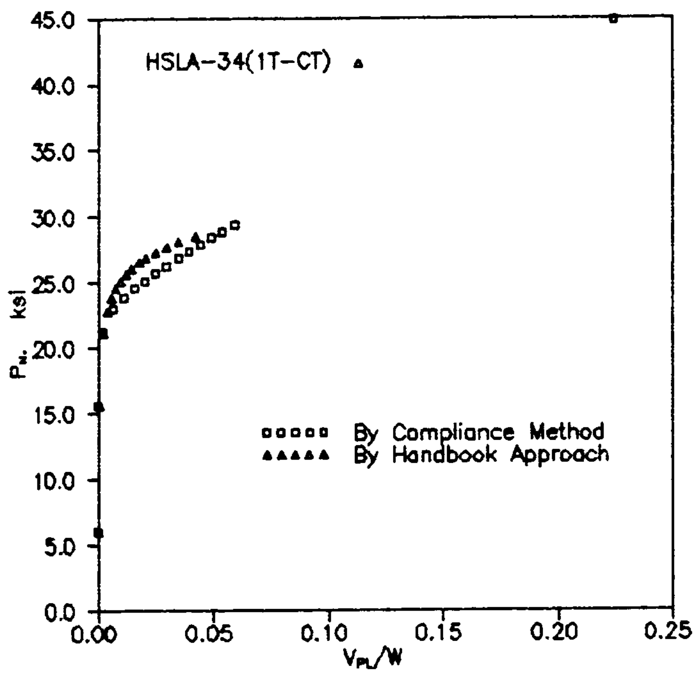

Fig. 11 The Beginning and Final Calibration Points Determined from the Handbook Approach for Specimen: HSLA-34

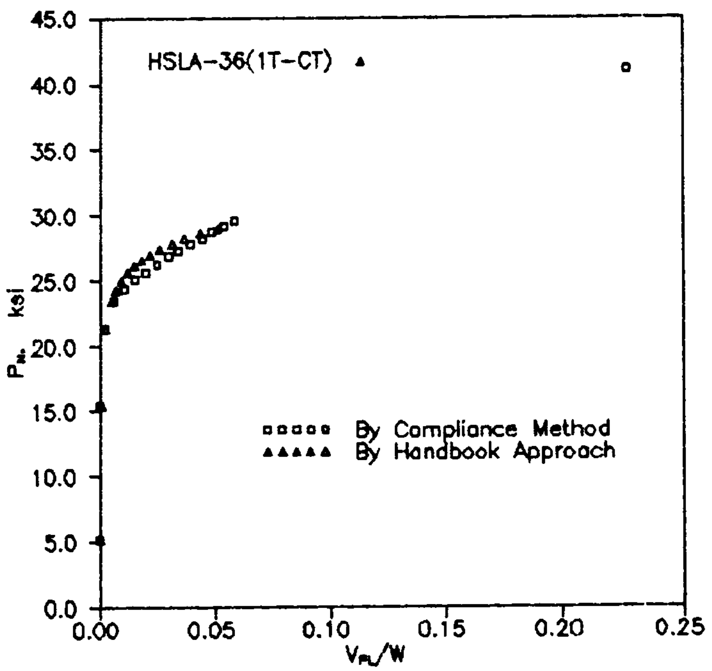

Fig. 12 The Beginning and Final Calibration Points Determined from the Handbook Approach for Specimen: HSLA-36

plastic load-line displacement (using Eq.(3.3)) when compared with corresponding results from compliance method. Therefore the indirect way, which uses Eq.(3.2) combined with Eq.(2.4) and (2.5) to evaluate J_{pl} first and then to calculate v_{pl}, will give a more accurate result of v_{pl} then the way which uses Eq.(3.3) to evaluate v_{pl} directly. The beginning calibration points given in Fig. 5 through Fig. 12 were evaluated from the indirect way and will be used to determine LMN function later.

Generally speaking, the beginning calibration points obtained by using the engineering Handbook approach are not so accurate, the error could be up to 30%. However, it seems that they would work for determining LMN functions, and only an approximately correct J-R curve result is expected.

3.3 Using an Empirical Formula to Obtain the Beginning Calibration Points

Landes and his group [36] had applied the LMN normalization method to analyze a number of test records, these tests were conducted previously using compact specimens which were made from different metallic materials and for size range from 1/2T (1 in. wide and 1/2 in thick) to 10T (20 in. wide and 10 in. thick). An LMN function was determined for each specimen. Based on the study of these LMN functions determined, it was found the constant L in the LMN function can be related to the material flow property and may best be expressed as a polynomial function of material flow stress by

$$L = -145.697 + 6.12795\sigma_y - 0.07702\sigma_y^2 + 0.0003370\sigma_y^3 \qquad (3.9)$$

where σ_y is give in ksi. The polynomial form for this was somewhat arbitrary chosen so an alternate form may also exist. The constant N varied in a very small range of $0.0005 < N < 0.001$. On the average it could be taken as a foxed constant for all the materials, in this study the value was chosen as

$$N = 0.0006 \qquad (3.10)$$

The constant M can then be determined from final calibration point by solving the combination of empirical formulas (3.9), (3.10) and Eq.(2.27). The LMN function determined from the empirical formula can be used to develop J-R curves directly, or for better results, used to obtain better beginning calibration points first and then the LMN function can be recalculated from three types of calibration points by the fitting procedure. In this study the latter approach was used.

Some sets of beginning calibration point obtained from above empirical formula approach are given in Fig. 13 through Fig. 18. From these results it can be seen that in most cases, such as the specimens made from A106, A533, HSLA or HY80 steels, this empirical formula approach can give a very good result for evaluating the beginning calibration points. But for some cases, such as the specimens made from A508 steel, the results were not so good. This may be due to the fact that the test specimens made from this material showed some variation in material flow properties. Eq.(3.9) was derived from the result of a statistical and numerical analysis. Some fitting error was involved in the procedure to form this equation in such a case.

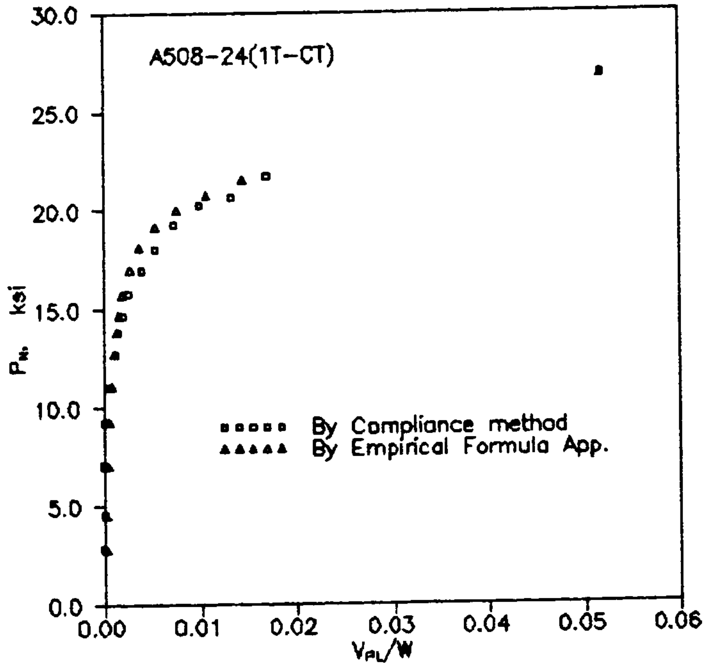

Fig. 13 The Beginning and Final Calibration Points Determined from the Empirical Formula Approach for Specimen: A508-24

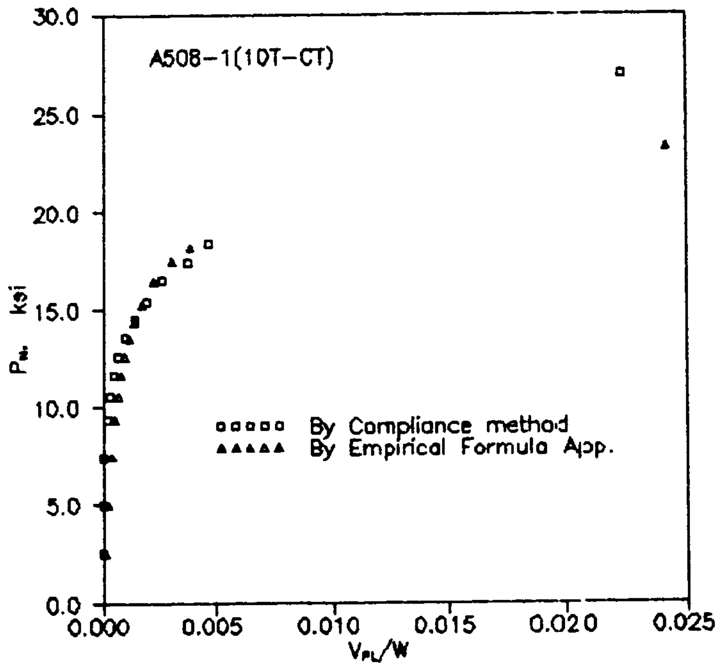

Fig. 14 The Beginning and Final Calibration Points Determined from the Empirical Formula Approach for Specimen: A508-1

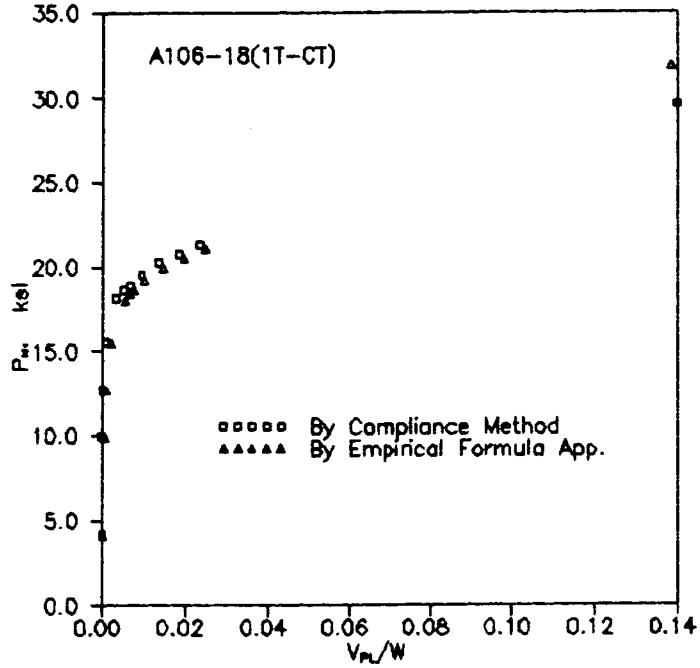

Fig. 15 The Beginning and Final Calibration Points Determined from the Empirical Formula Approach for Specimen: A106-18

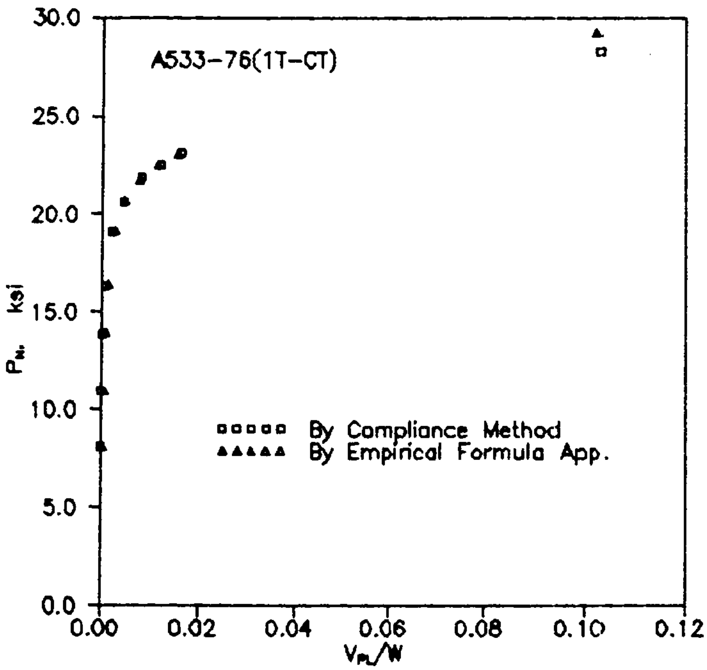

Fig. 16 The Beginning and Final Calibration Points Determined from the Empirical Formula Approach for Specimen: A533-76

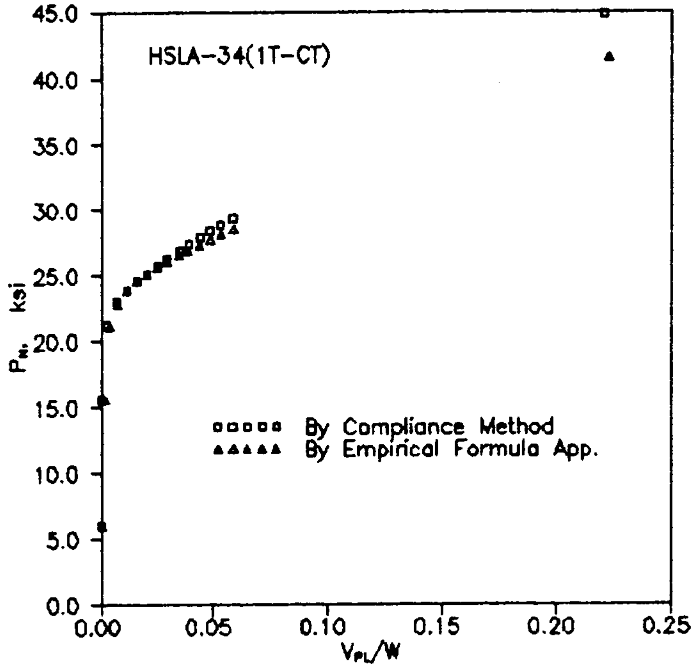

Fig. 17 The Beginning and Final Calibration Points Determined from the Empirical Formula Approach for Specimen: HSLA-34

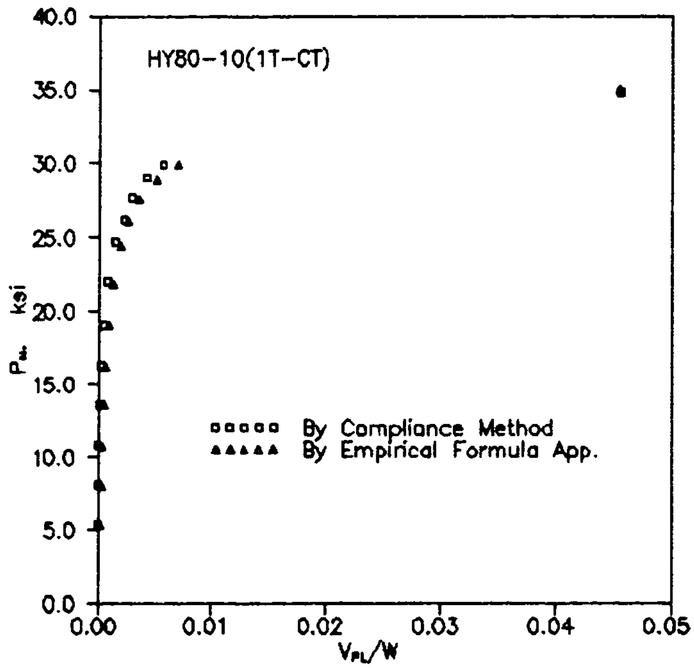

Fig. 18 The Beginning and Final Calibration Points Determined from the Empirical Formula Approach for Specimen: HY80-10

The value of the constant L is quite sensitive to a slight variation in the material flow stress when it is used to evaluate the beginning calibration points. Particularly, in this approach the same material flow stress was used to determine the L value for all specimens of the same material, hence the beginning calibration points for all the specimens made from this material would be identical. When there was material variability, this would result in variability in the beginning part of the normalized deformation curve. However, in general the beginning calibration points obtained from this approach are more satisfactory than those obtained from the first approach. Therefore a better result for developing J-R curves based on this approach would be expected.

3.4 Using a Power Law Assumption to Obtain the Beginning Calibration Points

In the early work of normalization, a pure power law was used to be the functional form of the normalized deformation function $H(v_{pl}/W)$ [15], that is

$$\frac{v_{pl}}{W} = \beta \, P_N^n \tag{3.11}$$

where n is same constant exponent used in the Ramberg-Osgood fit and β is a constant coefficient which reflects the material flow property. This functional form was applied successfully to describe the normalized deformation function $H(v_{pl}/W)$ and then to develop J-

R curves for materials that did not have extensive deformation during the fracture process. Also it should be noted that the introduction of the LMN function was based on the fact observed in a test specimen that the normalized deformation function $H(v_{pl}/W)$ appeared to have a power law character for small plastic displacement (v_{pl}/W) and a straight line character for large plastic displacement. These facts formed the idea of assuming a power law functional form to describe the normalized plastic deformation curve for evaluating the beginning calibration points.

In this study a reverse form of Eq.(3.11) was used, that is

$$P_N = \mu \left(\frac{v_{pl}}{W}\right)^{\kappa} \tag{3.12}$$

After a careful study of the normalized deformation functional behavior of a number of specimens made from different steels in this beginning region, it was found the exponent constant κ in Eq.(3.12) could be chosen as

$$\kappa = 0.13 \tag{3.13}$$

This exponent is valid only for describing the beginning segment of the normalized deformation curve. It appears to work provided a suitable value of the constant μ can be chosen for each metallic material. Some suitable values of constant μ for several different steels are given in Table 1.

Eq.(3.12) with κ = 0.13 and tabulated μ values in Table 1 has been applied to many specimens made from these materials to predict the beginning calibration points. Some results are shown in Fig. 19 through Fig. 30. These are also compared to the results from

Table 1 Some Suitable μ Values Chosen for Eq(3.12) when κ = 0.13

Material	σ_{ys} (ksi)	σ_{UTS} (ksi)	σ_y (ksi)	μ
A106 steel	47	81	64	34.8
A508 steel	56	79	67.5	36.0
A533 steel	64	87	75.5	39.0
HSLA steel	74	87	80.5	42.0
HY80 steel	89	106	97.5	58.0

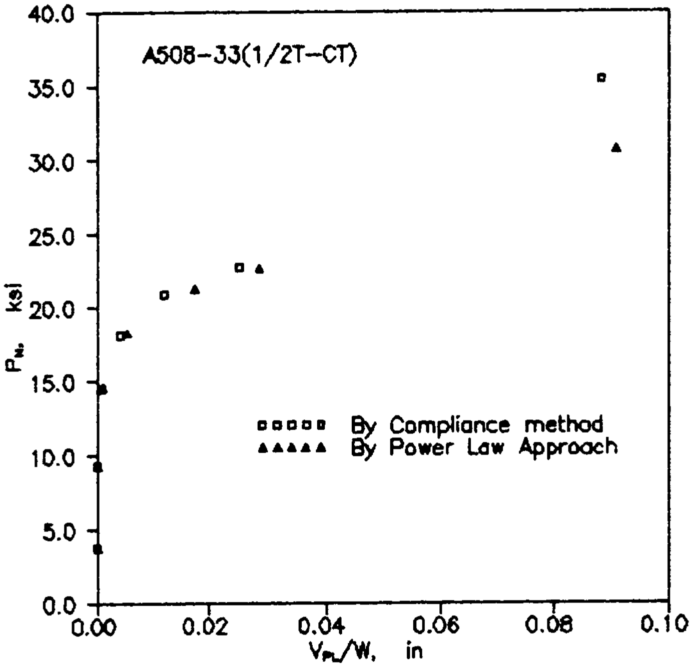

Fig. 19 The Beginning and Final Calibration Points Determined from the Power Law Approach for Specimen: A508-33

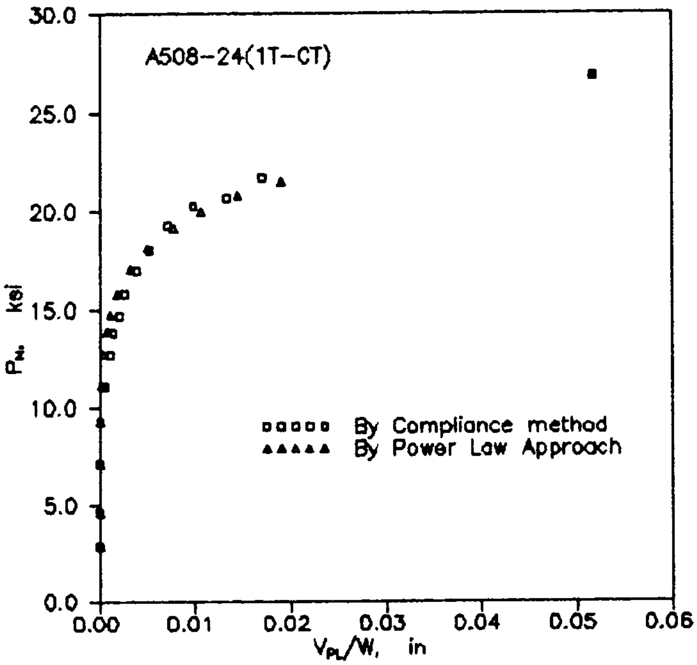

Fig. 20 The Beginning and Final Calibration Points Determined from the Power Law Approach for Specimen: A508-24

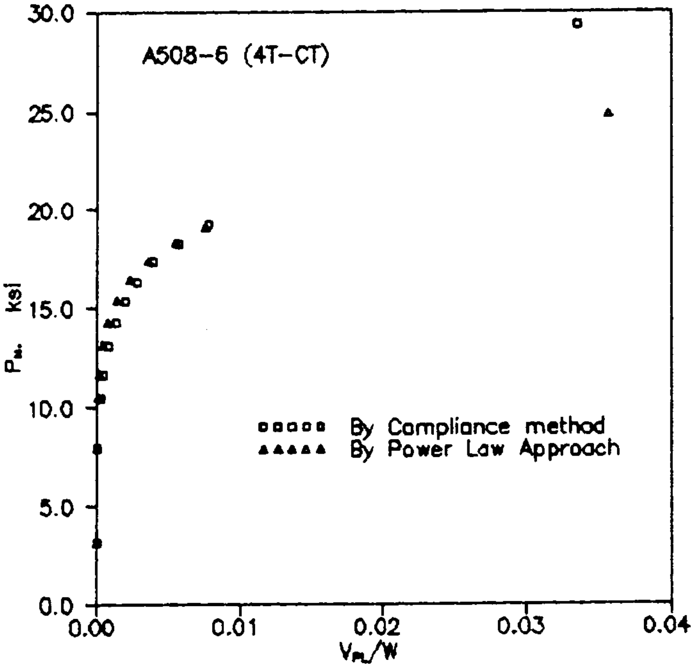

Fig. 21 The Beginning and Final Calibration Points Determined from the Power Law Approach for Specimen: A508-6

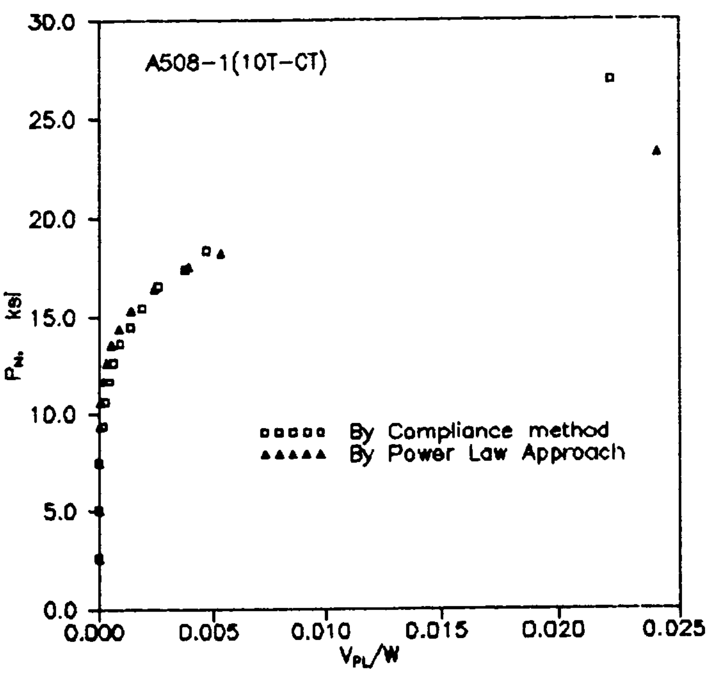

Fig. 22 The Beginning and Final Calibration Points Determined from the Power Law Approach for Specimen: A508-1

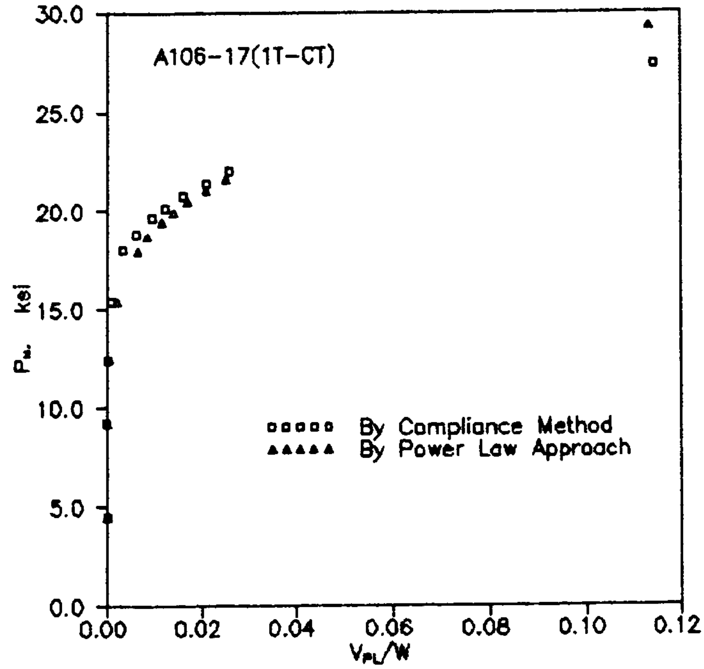

Fig. 23 The Beginning and Final Calibration Points Determined from the Power Law Approach for Specimen: A106-17

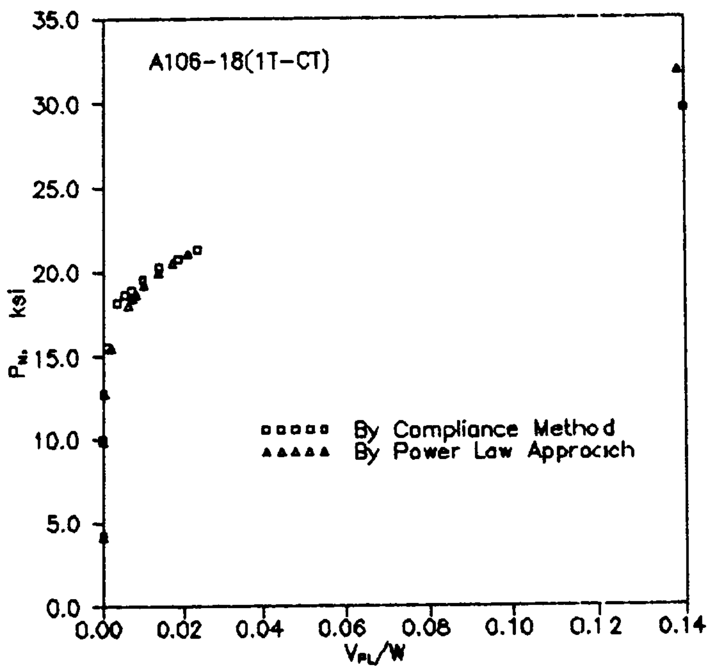

Fig. 24 The Beginning and Final Calibration Points Determined from the Power Law Approach for Specimen: A106-18

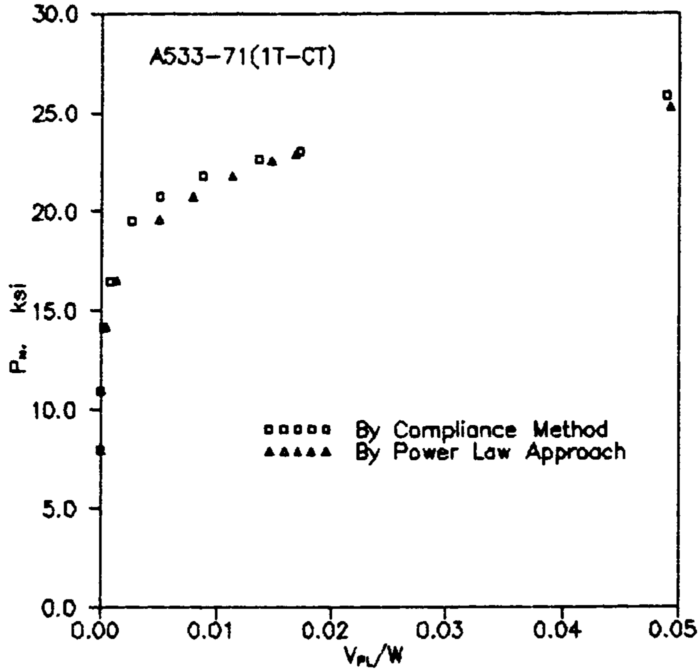

Fig. 25 The Beginning and Final Calibration Points Determined from the Power Law Approach for Specimen: A533-71

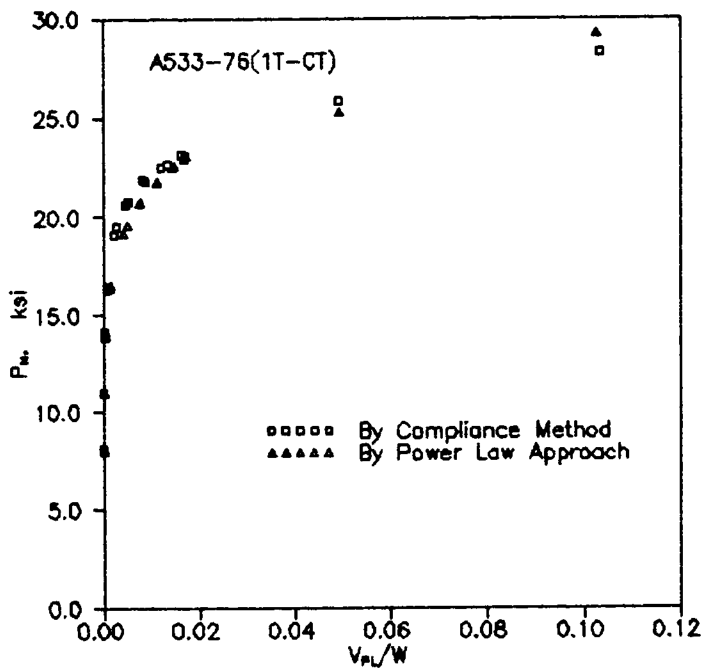

Fig. 26 The Beginning and Final Calibration Points Determined from the Power Law Approach for Specimen: A533-76

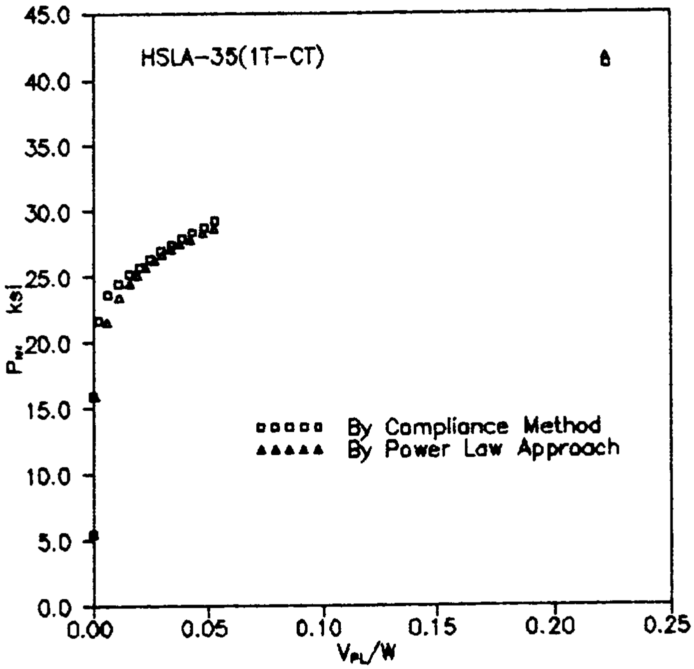

Fig. 27 The Beginning and Final Calibration Points Determined from the Power Law Approach for Specimen: HSLA-35

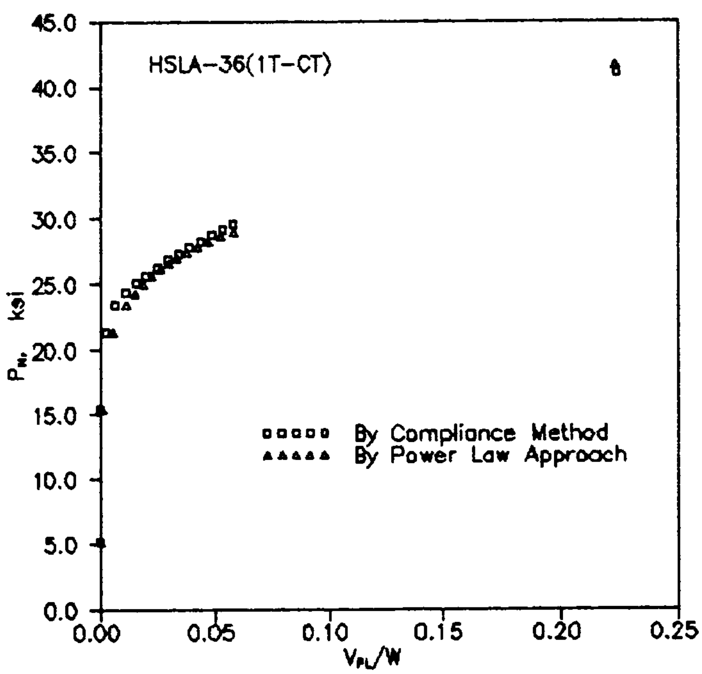

Fig. 28 The Beginning and Final Calibration Points Determined from the Power Law Approach for Specimen: HSLA-36

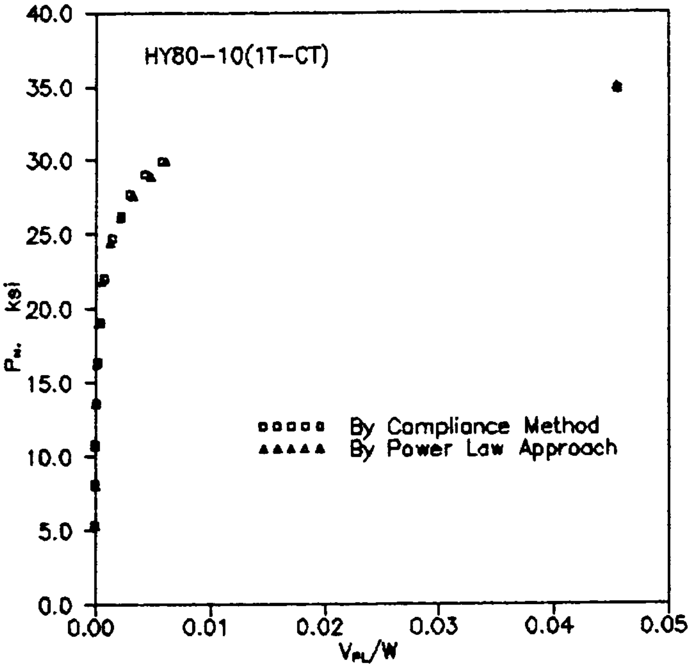

Fig. 29 The Beginning and Final Calibration Points Determined from the Power Law Approach for Specimen: HY80-10

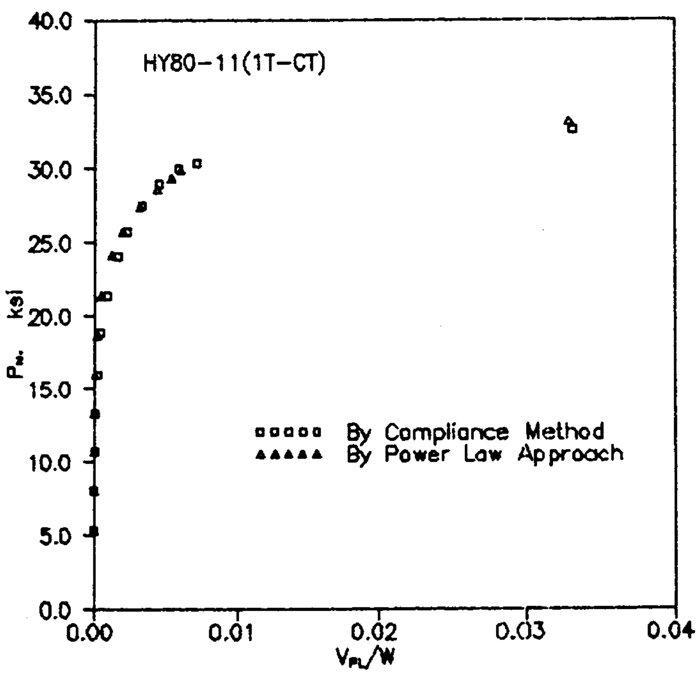

Fig. 30 The Beginning and Final Calibration Points Determined from the Power Law Approach for Specimen: HY80-11

the compliance method. From these results it can be seen that this approach worked successfully to predict the beginning calibration points for almost all the specimens evaluated here. These specimens had an extensive size range from 1/2T to 10T and the materials showed very different flow properties, including low strength, high toughness (such as A106 steel) to high strength, low toughness (such as HY80 steel). Based on these results used to determine LMN function then to develop J-R curve, a satisfactory result in developing the J-R curve would be expected.

It has been mentioned that the constant μ in Eq.(3.12) should reflect the material flow property. From the Table 1, it can be seen that the constant μ seems to be a function of the material flow stress σ_y. It could be expressed as a quadratic polynomial function of σ_y as follows

$$\mu = 67.619 - 1.33548\sigma_y + 0.012753\sigma_y^2 \tag{3.14}$$

The choice of this form is arbitrary and other alternate forms could also be found. The fitting result of μ versus σ_y was shown in Fig. 31. Eq. (3.12) through (3.14) can then be used to predict the beginning calibration points from the material flow properties. The results which were obtained by using Eq.(3.14) to determine μ then to evaluate the beginning calibration points from Eq.(3.12) and Eq.(3.13) were as good as the results given in Fig. 19 through Fig. 30. A great advantage of this approach is that the constant μ does not greatly influence the results, in that a small variation of the material

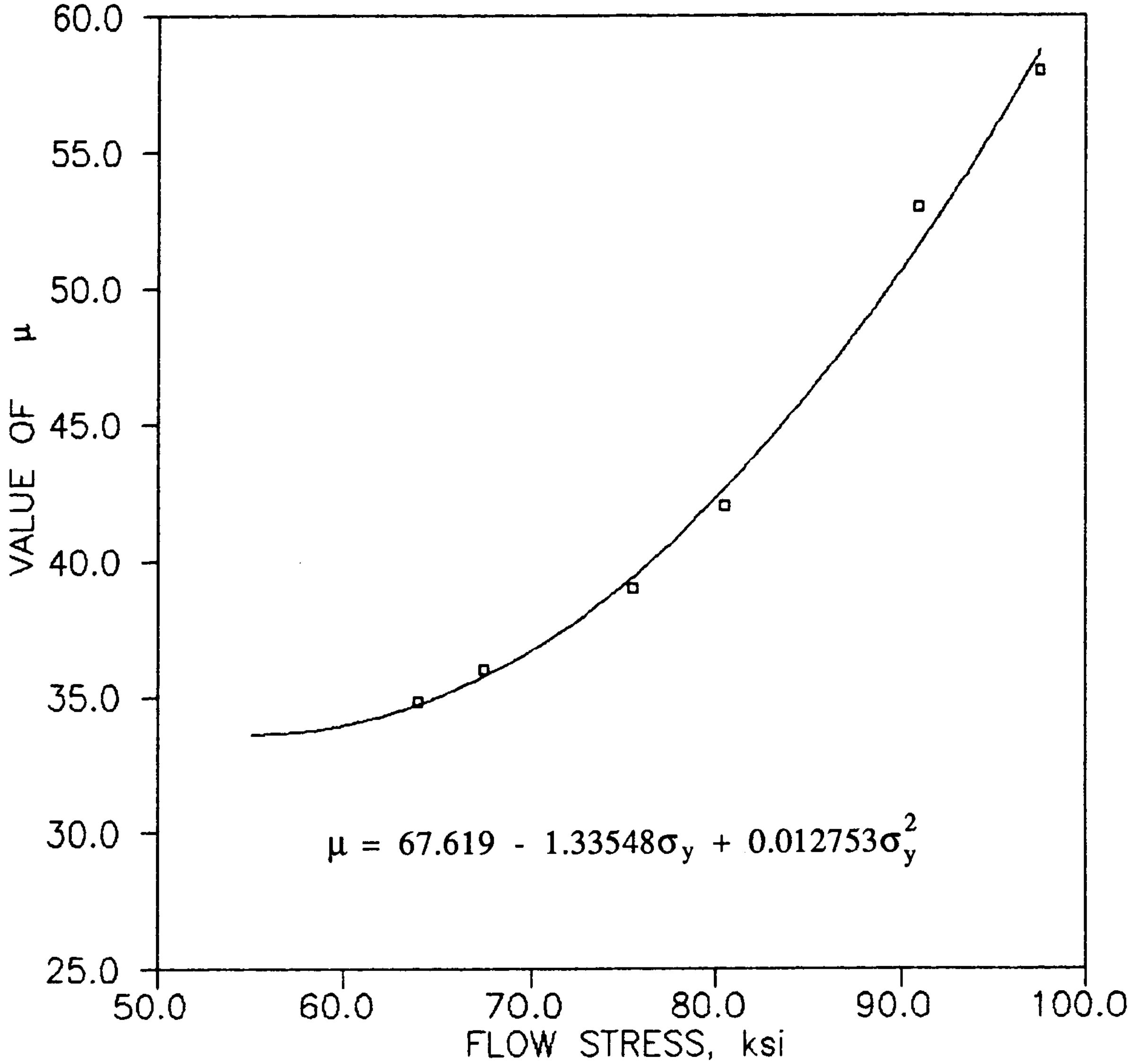

Fig. 31 The Quadratic Polynomial Fitting Result for μ in Eq.(3.12) Versus σ_y

flow stress does not change the resultant calibration very much. So this calibration is more accurate and versatile for developing J-R curves. The following section will describe how this approach can be used to develop J-R curves.

3.5 The Determination of LMN Function and the Evaluation of J

Once the beginning calibration points are obtained, the LMN function can be determined from the three types of calibration points, the predicted beginning calibration points, the intermediate calibration point which is fixed at $v_{pl}/W = 4.5\ \alpha\varepsilon_0$ and allowed to vary slightly in a range of P_N, and the final calibration point. The same fitting procedure described previously in section 2.2 can be used here for the determination of LMN function.

After the LMN function is determined, it specifies the load, plastic load-line displacement and crack length relationship uniquely. Then the plastic component of load-line displacement can be determined from the load versus crack length test record by solving the equation

$$P_N = \frac{P\ W}{Bb^2 g(b/W)} = \frac{[\ L + M(v_{pl}/W)\ ]\ (v_{pl}/W)}{N + (v_{pl}/W)} \qquad (2.27)$$

directly. Also the elastic component of load-line displacement can be determined from the compliance calibration function

$$C = \frac{1}{EB_e}\left(\frac{W+a}{W-a}\right)^2 \left[\, 2.1630 + 12.219(a/W) - 20.065(a/W)^2 - 0.9925(a/W)^3 + 20.609(a/W)^4 - 9.9314(a/W)^5 \,\right] \qquad (2.6)$$

for the compact specimen, or

$$C = \frac{1}{EB_e}\left(\frac{S}{W-a}\right)^2 \left[\, 1.193 - 1.908(a/W) + 4.478(a/W)^2 \quad 4.443(a/W)^3 + 1.739(a/W)^4 \,\right] \qquad (2.7)$$

for the three-point bend specimen,

with

$$v_{el} = PC$$

$$v = v_{el} + v_{pl}$$

Once the load-line displacement is determined, it can be used with the load versus crack length record to develop the J-R curve. This can be done by integrating the deformation function directly [33] or by using the Eq.(2.3) through Eq.(2.13) in the E1152 standard test method.

4. APPLICATION RESULTS, DISCUSSION AND CONCLUSIONS

4.1 Application Results

The three approaches proposed in the previous section are used along with the LMN normalization method to develop J-R curves from only the load versus crack length records. The input information can be developed by conducting tests in a manner similar to the ASTM E813 and E1152 standard test methods except that a displacement measurement is not used. The D. C. potential drop method is recommended to be used for obtaining the load versus crack length record. The calibration for determining LMN function requires a physically measured initial and final crack length as well as the final plastic load-line displacement which can be estimated from a measurement of permanent plastic deformation in the specimen at the end of the test. The methods in ASTM E813 and E1152 for measuring crack length are recommended. For more reliable and satisfactory results some additional information about the material tensile properties are also needed.

These three approaches along with the LMN normalization method have been applied to many test specimens to develop J-R curves from load versus crack length records. These tests had previously been conducted and analyzed to develop J-R curves using the elastic compliance method as well as using the LMN normalization method from the load versus displacement pairs without the use of a crack length measurement.[37, 38, 17]. Some of these results are given in Fig. 32 through Fig. 53* to illustrate how these three approaches used along with the LMN normalization method work. All these results are compared with both earlier results analyzed by the elastic compliance method and analyzed by the LMN normalization method from load versus displacement records. The third approach, the power law approach, is emphasized because it worked more successfully to predict the beginning calibration points for different specimens analyzed. Only a few results are given here for the first and second approach, but it is enough to get the idea of how successfully these methods work.

Fig. 32 through Fig. 34 show the application results from the Handbook approach. Fig. 32 shows a successful case for specimen A508-24. The result for specimen A508-6 shown in Fig. 33 is not so satisfactory. Fig. 34 represents a bad case for this approach, a large error appeared for specimen A106-17. Other application results for specimens made from A106, A533, HSLA, HY80 steel are also not so good. This may be due to the fact that full tensile properties were not available and the Bloom method for evaluating the material hardening constants α and n was used. A considerable error was introduced into the beginning calibration points by constants α and n from the Bloom method. If the values of material hardening constants, α and n, from true stress-true strain are used, the results could be improved.

---

* Figures 32 through 53 may be found in the Appendix

Fig. 35 through Fig. 37 show the results from the empirical formula approach for the same specimens shown in Fig.32 through Fig. 34. Fig. 37 shows a satisfactory result for specimen A106-17. Many other results from this approach for specimens made from A106, A533, HSLA steel are as good as this. The results shown in Fig.35 and Fig. 36 are not so satisfactory, These are the cases for the specimens made from A508 steel. It has been mentioned in previous section that this material showed variable flow properties for each specimen. In this study the same flow stress σ_y was used to predict the beginning calibration points for all the specimens made from the same material. This may not have been correct for some of the specimens made from the 508 steel. If the true flow stress is used for each specimen, the results could be improved.

The results from the power law approach along with the LMN normalization method, named as the power law-LMN normalization method, are shown in Fig. 38 through Fig. 53. Five specimen size were included, 1/2T-CT, 1T-CT, 2T-CT, 4T-CT, and 10T-CT (where the number in front of T corresponds to thickness in inches and each specimen had a width equal to twice the thickness, the CT is referred to the compact specimen). Results were developed for test specimens which made from five different materials, A508, A106, A533, HSLA and HY80 steel. Almost all the results showed a good agreement with the results developed by the elastic compliance method and developed by the LMN normalization method from the load versus displacement records.

Fig. 38 through Fig. 43 show results for an A508 vessel steel [37] for the size range from 1/2T to 10T. The first and second approach did not work so good for this material. The results given here show the power law approach worked much more better, although the same flow stress was used to predict the beginning calibration points for determining the LMN function for the specimens made from the same material. This demonstrates that this power law approach is more accurate and versatile.

Fig. 44 and Fig. 45 are for an A106 steel [38]. This is the case for a low strength and high toughness material. The power law-LMN normalization method successfully developed the J-R curves for this material. Fig. 45 shows that this approach maintains some of the advantages of the normalization method, i.e. the negative slope at the end of the J-R curve from the elastic compliance method can be removed by normalization method.

Fig. 46 and Fig. 47 show the satisfactory results obtained for an A533 steel from this new method.

Fig. 48 through Fig. 50 show the results for an HSLA steel [38]. The HSLA material has the most plastic deformation of all materials studied. The J-R curves analyzed previously by the LMN normalization method from the load versus displacement records for this material had shown the worst agreement with the elastic compliance method for all cases studied [17]. In contrast here, Fig. 48 through Fig. 50 show that the results analyzed by the power law-LMN normalization method from load versus crack length records were improved, a better agreement is shown between the results analyzed by the elastic compliance method and by the new method.

Fig. 51 through Fig. 53 are for an HY80 steel [38]. This material has high strength and low toughness. This is a difficult case for developing J-R curves from the load versus crack length records, Because the plastic deformation is so small and therefore harder to predict, a slight error of the predicted plastic displacement measurement will cause large deviation in J-R curve result. However, the results from the power law-LMN normalization method look good for test specimens of HY80-10 in Fig. 51 and HY80-12 in Fig. 53. The result for HY80-11 test specimen in Fig. 52 represents the worst case of all presented in this study, however, even this result could be judged to be acceptable.

4.2 Discussion and Conclusions

The three approaches proposed here along with the LMN normalization method enable J-R curves to be developed from the load versus crack length records. These approaches use the material flow properties to predict several points in the beginning segment of the deformation curve for constructing the LMN function. Then using the normalization method and the ASTM E1152 standard test method J-R curves can be developed. In cases were the material shows variable flow properties for different individual specimen, it is recommended that the true material flow properties from the tensile test be used.

The results given in Fig. 32 through Fig. 53 show that the first approach, that of using Handbook calibration curves, can work for developing J-R curves from load versus crack length records. However, the results from this approach are often not very exact. The second approach, that of using an empirical calibration formula, worked better than the first one. But in some cases, such as for A508 steel, it did not worked so satisfactory. The third approach, using the power law, worked best. This approach combined with the LMN normalization method gave the best results. This method worked satisfactorily for an extensive range of specimen sizes and various metallic materials which have very different properties. The accuracy of the results from this new method is as good as the results from the elastic compliance method.

It should be mentioned here that an important advantage of the normalization method is the fact that the normalized plastic deformation curves from different test specimens which are made from the same material seem to have the same behavior at the beginning range of v_{pl}/W, although the material may show a small variation of material flow properties for each specimen. This is illustrated in Fig. 54** for some A508 steel specimens which have the size range of 1/2T to 10T. The power law approach takes the advantage of this and uses the material flow properties to predict some calibration points at this beginning segment of the normalized

---

** Figure 54 may be found in the Appendix plastic deformation curve; this is one reason why it can work so successfully. The power law-LMN normalization method also maintains almost all of advantages of the LMN normalization method, for example, because the physical final crack length measurement is used, the new method can also correct the error at the end segment of the J-R curves analyzed by the elastic compliance method, where the crack monitoring system may fail to accurately predict the final crack length. In such a case the normalization method appears to give better results. This can be seen from the Fig. 38, 42, 43, 45, and Fig. 48 etc. . It may be noted that the J-R curves developed by the power law-LMN normalization method from the load versus crack length records for a lower strength and higher toughness material were better than those for a higher strength and lower toughness material. This is due to the fact that the lower strength and higher toughness material has a larger plastic deformation which could be predicted more accurately in terms of relative error. More care must be taken for the high strength and low toughness material when the J-R curves are analyzed from load versus crack length records. In such cases the true material flow stresses are recommended to be used for individual specimens in using the power law-LMN normalization method.

Based on above facts the power law approach along with LMN normalization method could be judged to be a successful method for developing J-R curves from load versus crack length records without a displacement measurement. It could offer a great advantage for developing J-R curves in restrictive facilities such as a hot cell or at high temperature. As an overall assessment of this method, it appears satisfactory for use with the ASTM standards and could be offered as a candidate to incorporate into the standards for conducting and analyzing J-R curve test in some special cases. However, before it could be adopted by consensus, experience and further evaluation are needed. Therefore it is recommended to the readers who are interesting in this new method to use it in the practical tests.

BIBLIOGRAPHY

BIBLIOGRAPHY

[1] Rice, J. R., " A Path Independent Integral and the Approximate Analysis of Strain Concentration by Notches and Cracks", Journal of Applied Mechanics, 35, 1968, pp. 379-386

[2] Hutchinson, J. W., " Singular Behavior at the End of Tensile Crack in a Hardening Material", Journal of the Mechanics and Physics of Solids, Vol. 16, 1, 1968, pp. 13-31

[3] Hutchinson, J. W., " Plastic Stress and Strain Fields at a Crack Tip", Journal of the Mechanics and Physics of Solids, Vol. 16, 5, 1968, pp. 337-347

[4] Rice, J. R., " Mathematical Analysis in the Mechanics of Fracture", in Fracture Vol. II, H. Liebowitz, Ed., Academic Press, 1968, pp. 191-311

[5] Begley, J. A. and Landes, J. D., " The J Integral as a Fracture Criterion", in Fracture Toughness, ASTM STP 514, American Society for Testing and Materials, 1972, pp. 1-23

[6] Begley, J. A. and Landes, J. D., " Serendipity and the J Integral", International Journal of Fracture, Vol. 12, 5, 1976

[7] Landes, J. D. and Begley, J. A., in Fracture Analysis ASTM STP 560, American Society for Testing and Materials, 1974, pp. 170-186

[8] Heyer, R. M. and McCabe, D. E., " Crack Growth Resistance in Plane Stress Fracture Testing", Engineering Fracture Mechanics 4, 1972, pp. 413-430

[9] McCabe, D. E. and Heyer, R. H., " R Curve Determination Using a Crack-line Wedge Loaded(CLWL) Specimen", ASTM STP 527, American Society for Testing and Materials, 1973, pp. 17-35

[10] Paris, P. C., Tada, H. , Zahoor, A. and Ernst, H. , "Instability of the Tearing Mode of Elastic-Plastic Crack Growth," ASTM STP 668, American Society for Testing and Materials, 1979, pp. 5-36.

[11] Paris, P. C. , Tada, H. , Ernst, H. and Zahoor, A. , "An Initial Experimental Investigation of the Tearing Instability Theory," ASTM STP 668, American Society for Testing and Materials, 1979, pp256-265.

[12] "Standard Test Method for J_{Ic}, A Measure of Fracture Toughness," ASTM Method E813, 1987 ASTM Book of Standards, Vol. 03. 01

[13] "Standard Test Method for Determine J-R Curve," ASTM Method E1152, 1987 ASTM Book of Standard, Vol. 03. 01

[14] Landes, J. D. and Herrera, R. , " A New Look at J-R Curve Analysis," International Journal of Fracture, Vol. 36, 1988, pp R9-R14

[15] Herrera, R. and Landes, J. D. , " A Direct J-R Curve Analysis of Fracture Toughness Test," Journal of Testing and Evaluation, JTEVA, VOL. 16, No. 5, Sept. 1988, pp 427-449.

[16] Herrera, R. and Landes, J. D. , " Direct J-R Curve Analysis: A Guide to the Methodology," presented at the 21st National Symposium on Fracture Mechanics, Annapolis, Maryland, June 28-30, 1988.

[17] Zhou, Z. , Herrera, R. , Lee, K. and Landes, J. D. , " Normalization: An Experimental Method for Developing J-R Curves ", presented at the Second Symposium of User Experience on Elastic-Plastic Fracture Toughness Test Methods, ASTM, Lake Buena Vista, FL, November 1989.

[18] Joyce, J. A. , Ernst, H. and Paris, P. C. , " Direct Evaluation of J-Resistance curves from Load Displacement Records," in Fracture Mechanics: Twelfth Conference, ASTM STP 700, American Society for Testing and Materials, Philadelphia, 1980, pp222-236.

[19] Landes, J. D. and Begley, J. A. , " The Effect of Specimen Geometry on J_{Ic}," in Fracture Toughness, ASTM STP 514, American Society for Testing and Materials, 1972, pp24-39.

[20] Bucci, R. J. , Paris, P. C. , Landes, J. D. and Rice, J. R. , "J Integral Estimation Procedures," in Fracture Toughness, ASTM STP 514 American Society for Testing and Materials, 1972, pp. 40-70.

[21] Rice, J. R. , Paris, P. C. and Merkle, J. G. , " Some Further Results of J-Integral Analysis and Estimates, " ASTM STP 536, American Society for Testing and Materials, 1973.

[22] Clarke, G. A. , Andrews, W. R. , Paris, P. C. and Schmidt, D. W. , " Single Specimen Test for J_{Ic} values Determination," in Mechanics of Crack Growth, ASTM STP 590, American Society for Testing and Materials, 1976, pp. 27-42.

[23] Ernst, H. A. , Paris, P. C. and Landes, J. D. , " Estimation of J-Integral and Tealing Modules T from a Single Specimen Test Record," in Fracture Mechanics: Thirteenth Conference, ASTM STP 743, American Society for Testing and Materials, 1981, pp. 476-502.

[24] Hudak, S. J. and Saxena, A. , "Review and Extension of Compliance Information for Common Crack Growth Specimens," International Journal of Fracture, Vol.14, No. 5, Oct. 1978, pp. 453-468.

[25] " Recommended Practice for R Curve Determinations," ASTM Annual Book of Standard Part 10, American Society for Testing and Materials, Philadelphia, 1975.

[26] Joyce, J. A. and Gudas, J. P. , " Computer Interactive J_{Ic} Testing of Navy Alloys," in Elastic-Plastic Fracture, ASTM STP 668 American Society for Testing and Materials, 1979, pp. 451-468

[27] Orange, T. W. , " Method and Models for R-Curve Instability Calculations," Presented at 21st National Symposium on Fracture Mechanics, Annapolis, MD. June, 1988.

[28] Ernst, H. A. , Paris, P. C. , Rossow, M. and Hutchinson, J. W. , " Analysis of Load Displacement Relationship to Determine J-R Curve and Tearing Instability Material Properties," in Fracture Mechanics, ASTM STP 667, American Society for Testing and Materials, 1979, pp. 581-599

[29] Ernst, H. A. and Paris, P. C. , " Techniques of Load-Displacement by J-Integral Methods, " NUREG/CR-1222, Nuclear Regulatory Commission, Jan. 1980.

[30] Sharobeam, M. H. and Landes, J. D. , " The Separation Criterion and Methodology in Ductile Fracture Mechanics," (Submitted for Publication)

[31] Sharobeam, M. H. and Landes, J. D. , " Eta Factor in Elastic-Plastic Fracture Testing," Presented at the Second Symposium on User Experience with Elastic-Plastic Fracture Test Method, ASTM, November, 9, 1989, Lake Buena Vista, FL.

[32] Landes, J. D. and Herrera, R. , Unreported Results.

[33] Landes, J. D. , Herrera, R. , Lee, K. and Zhou, Z. , " The LMN Normalization Method for J-R Curve Analysis," (To be submitted for publication).

[34] Kumar, V. , German, M. D. and Shih, C. F. , " An Engineering Approach for Elastic-Plastic Fracture Analysis," Electrical Power Research Institute, NP1931. Topical Report , July 1981.

[35] Tada, W. , Paris, P. C. and Irwin, G. R. , " The Stress Analysis of Cracks Handbook," Del Research Corporation, Hellertown, Pa. , 1973

[36] Zhou, Z. , Landes, J. D. and Lee, K. , Unreported Results

[37] Landes, J. D. , McCabe, B. E. and Ernst, H. A. , " Fracture Testing of Ductile Steels," Electrical Power Research Institute, MP-5401, Final Report of Project 1238-2, Jan. , 1987.

[38] Joyce, J. A. , Davis, D. A. , Hays, R. A. and Hacktt, E. H. , " Application of the J-Integral and Modified J-Integral to Cases of Large Crack Extension," NUREG CR-5143, Feb., 1989.

[39] Bloom, J. M. , " Determination of the Ramberg-Osgood Constants," ASME Section XI Pipe Flaw Evaluation Group, Nov. , 1985.

APPENDIX

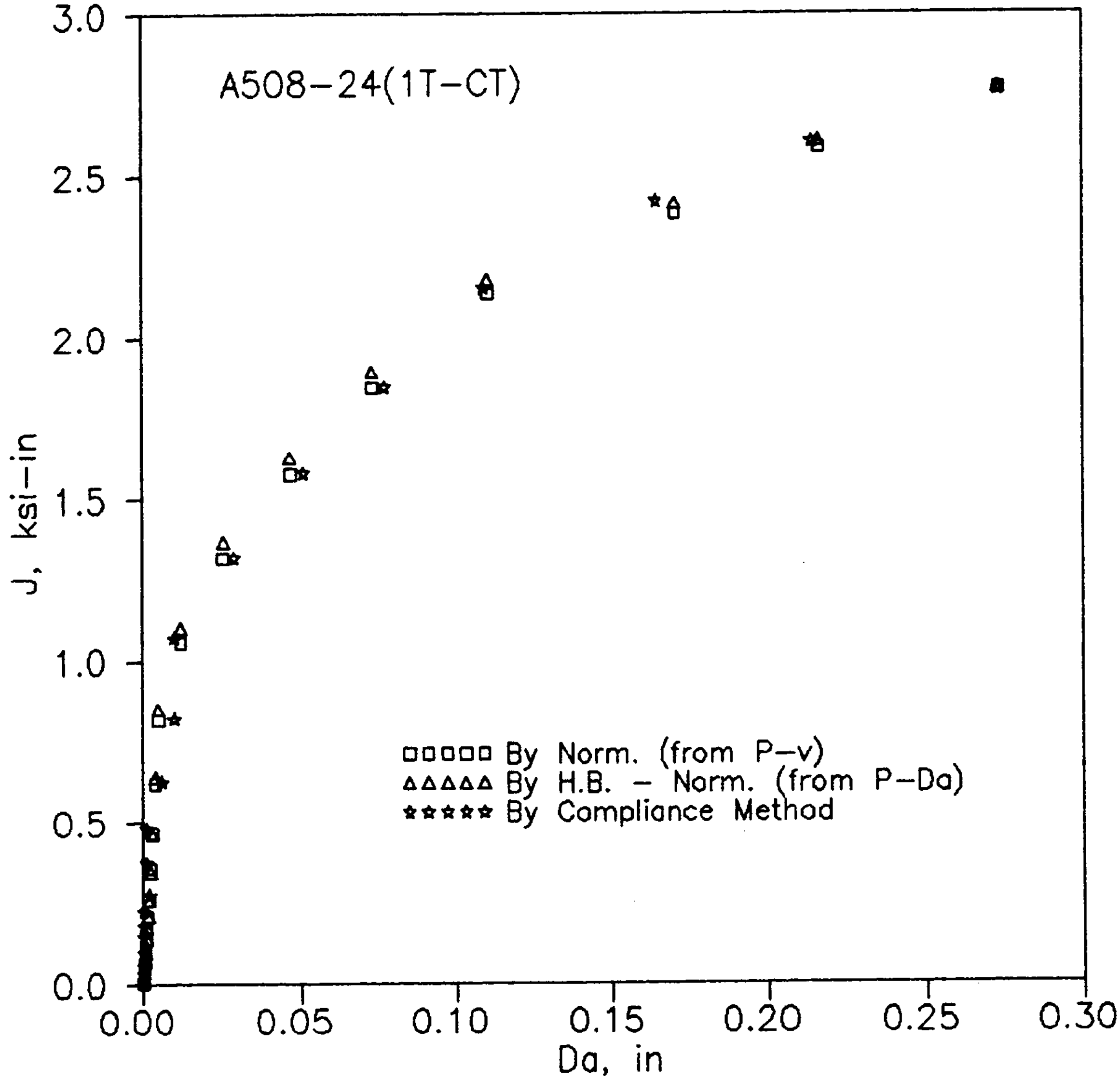

Fig. 32 J-R Curve from Handbook Approach for Specimen A508-24

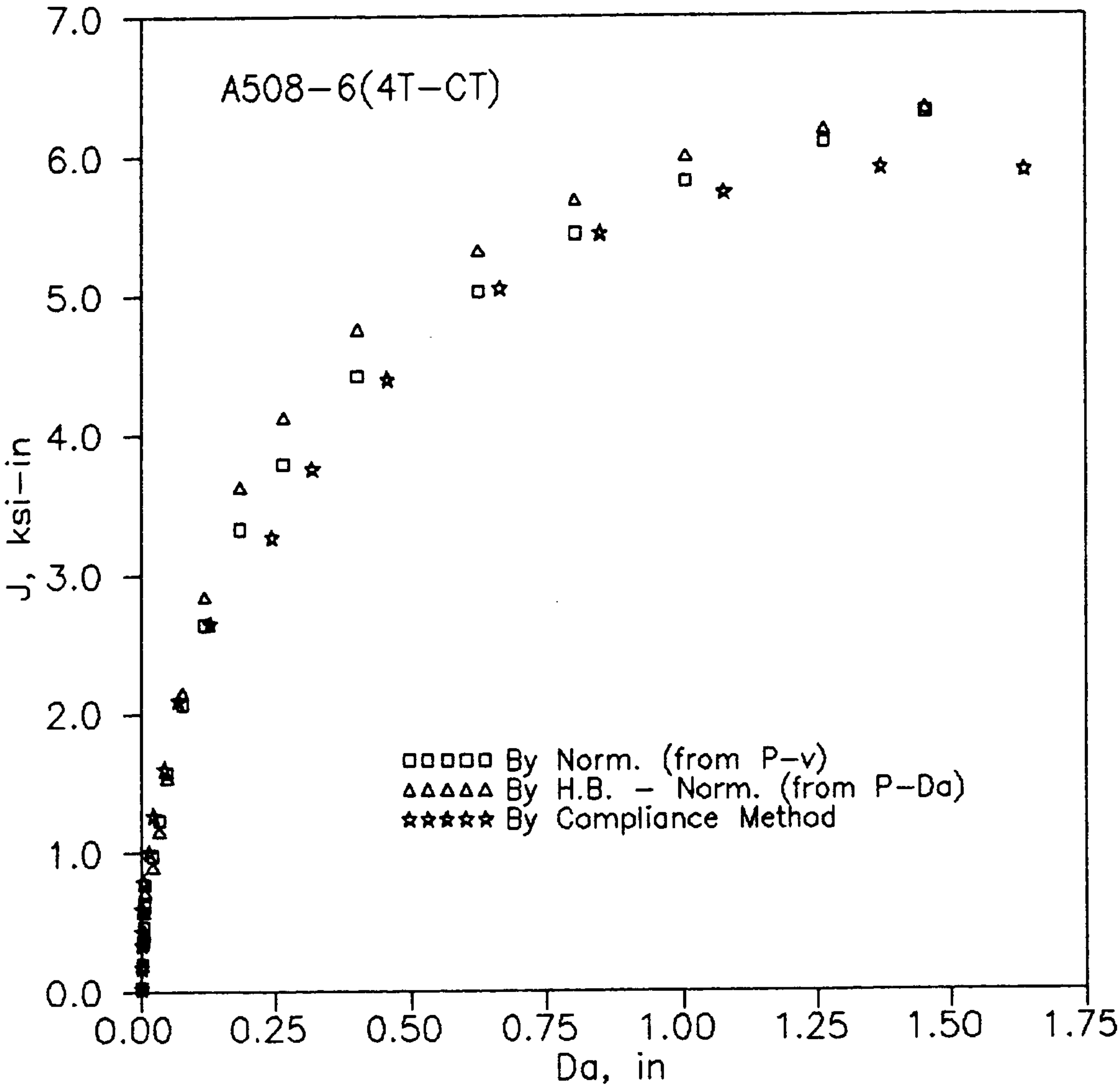

Fig. 33 J-R Curve from Handbook Approach for Specimen A508-6

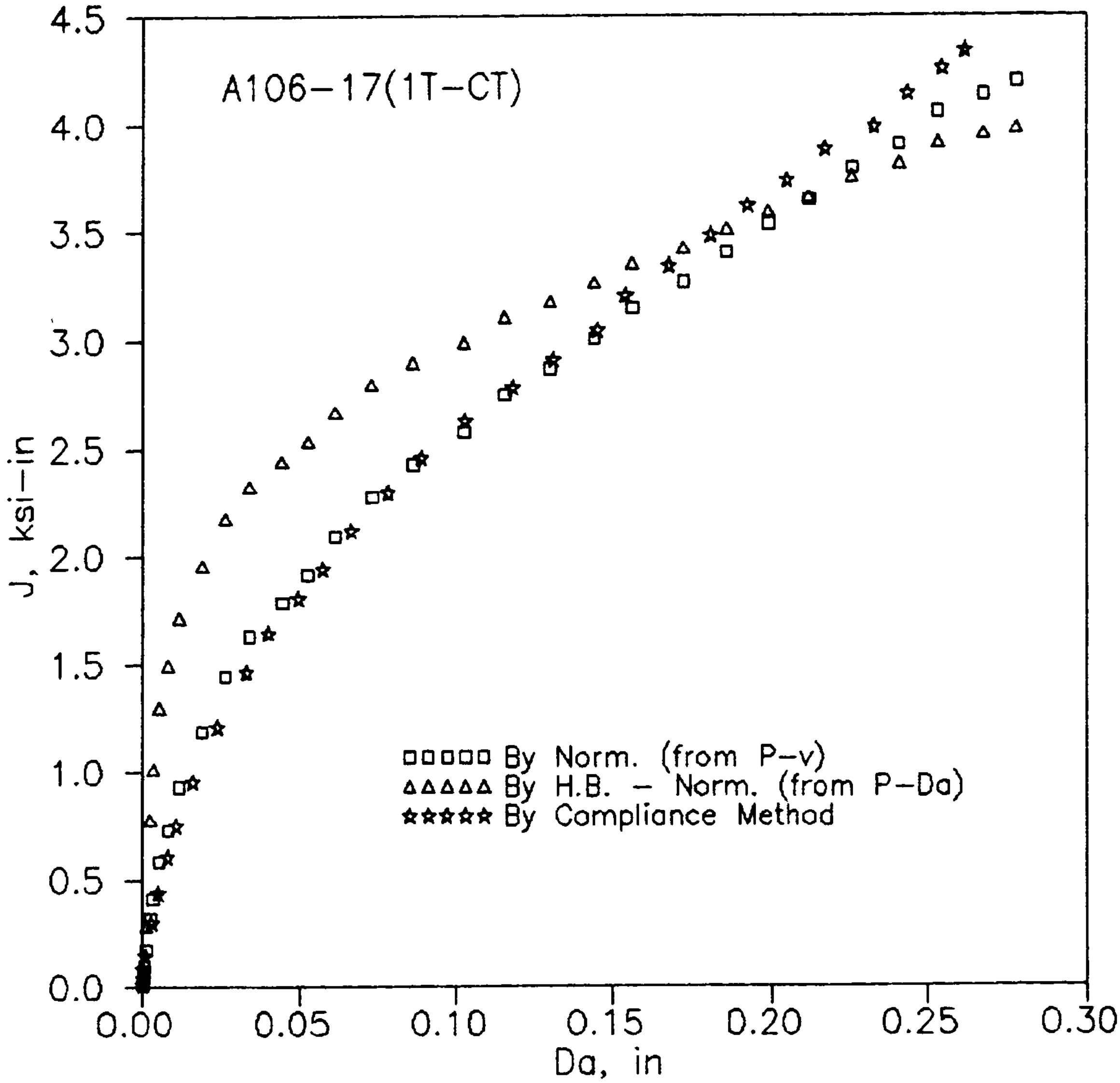

Fig. 34 J-R Curve from Handbook Approach for Specimen A106-17

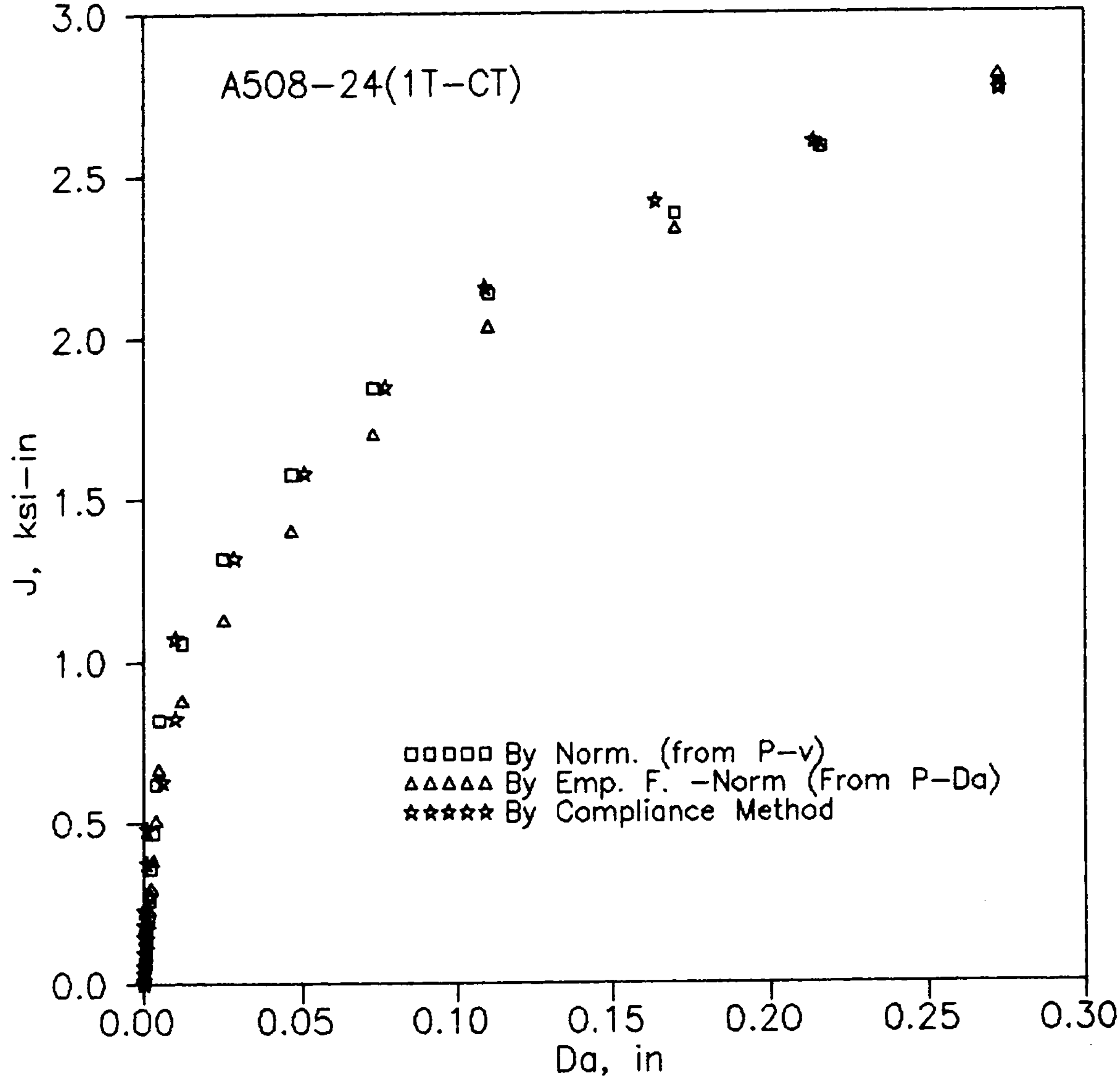

Fig. 35 **J-R Curve from Empirical Formula Approach for Specimen A508-24**

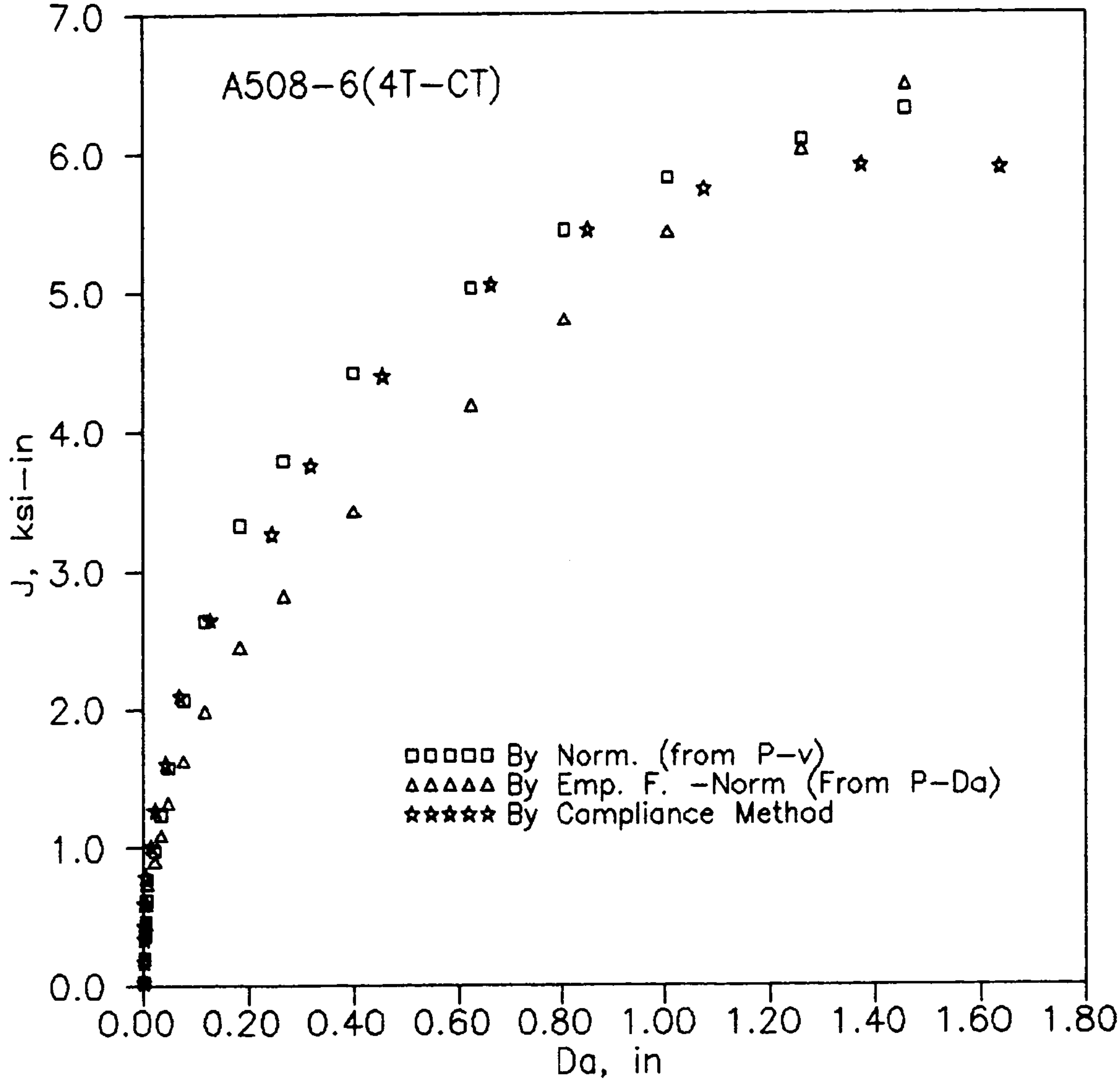

Fig. 36 J-R Curve from Empirical Formula Approach for Specimen A508-6

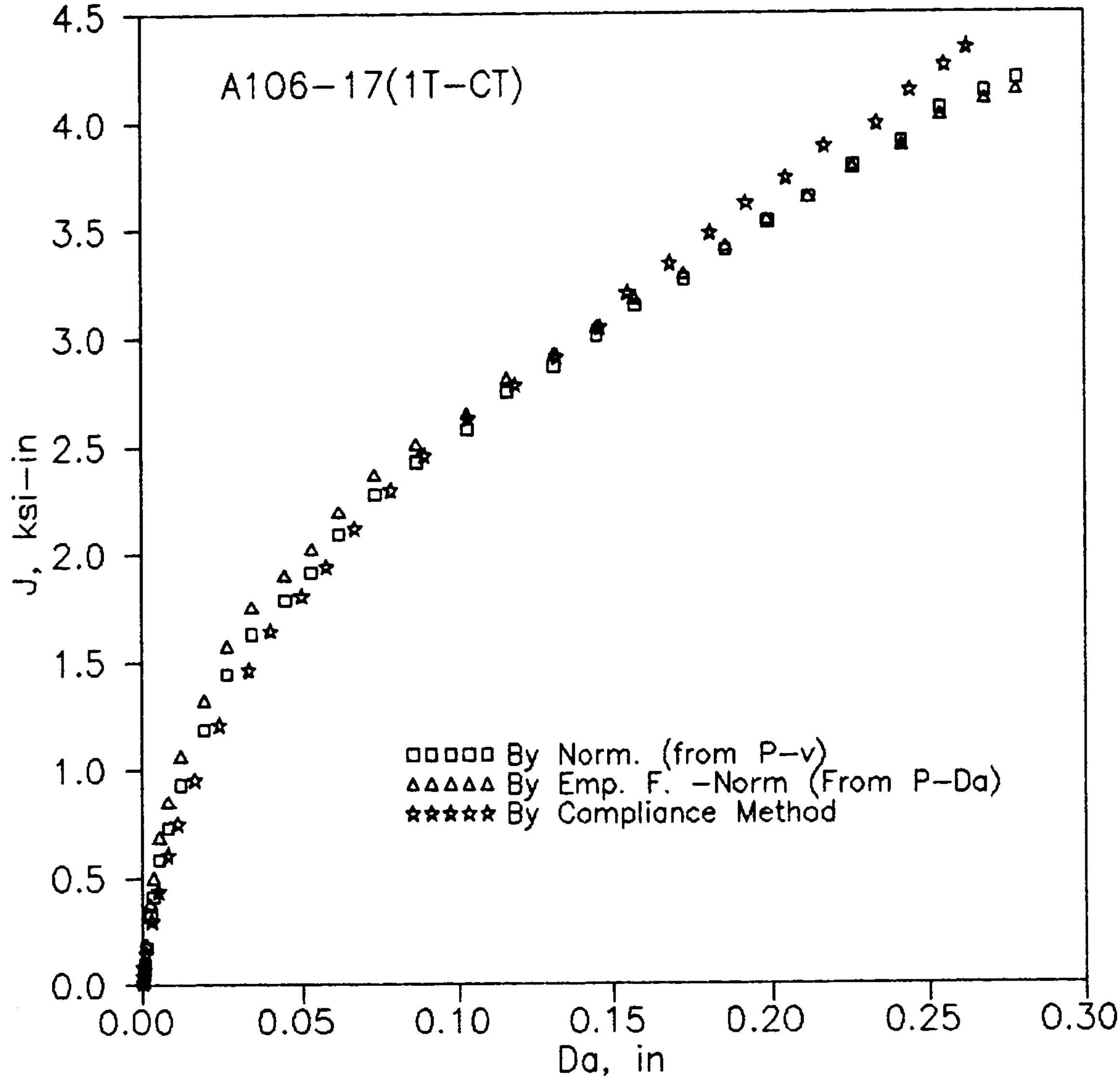

Fig. 37 J-R Curve from Empirical Formula Approach for Specimen A106-17

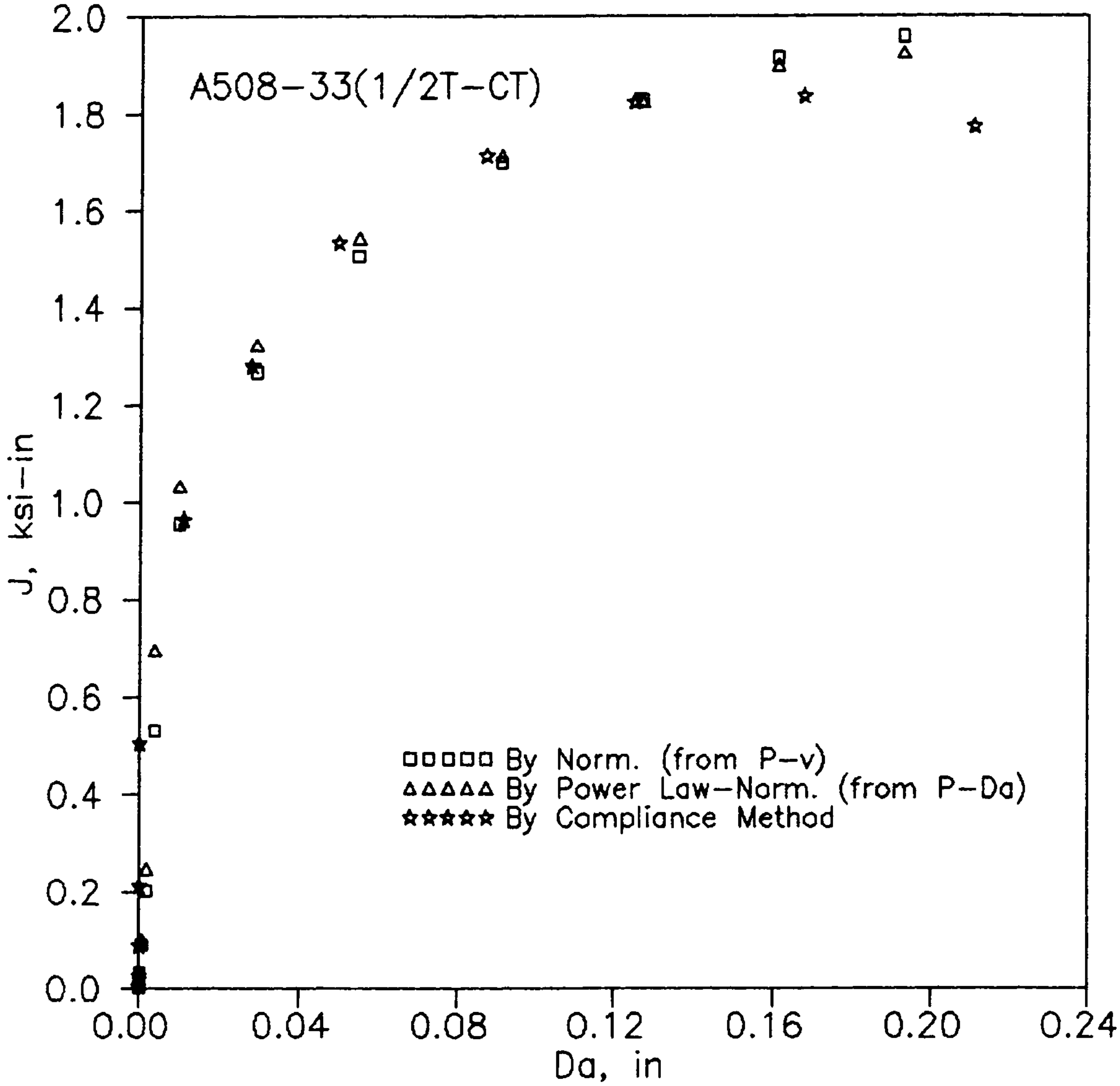

Fig. 38 J-R Curve from Power Law Approach for Specimen A508-33

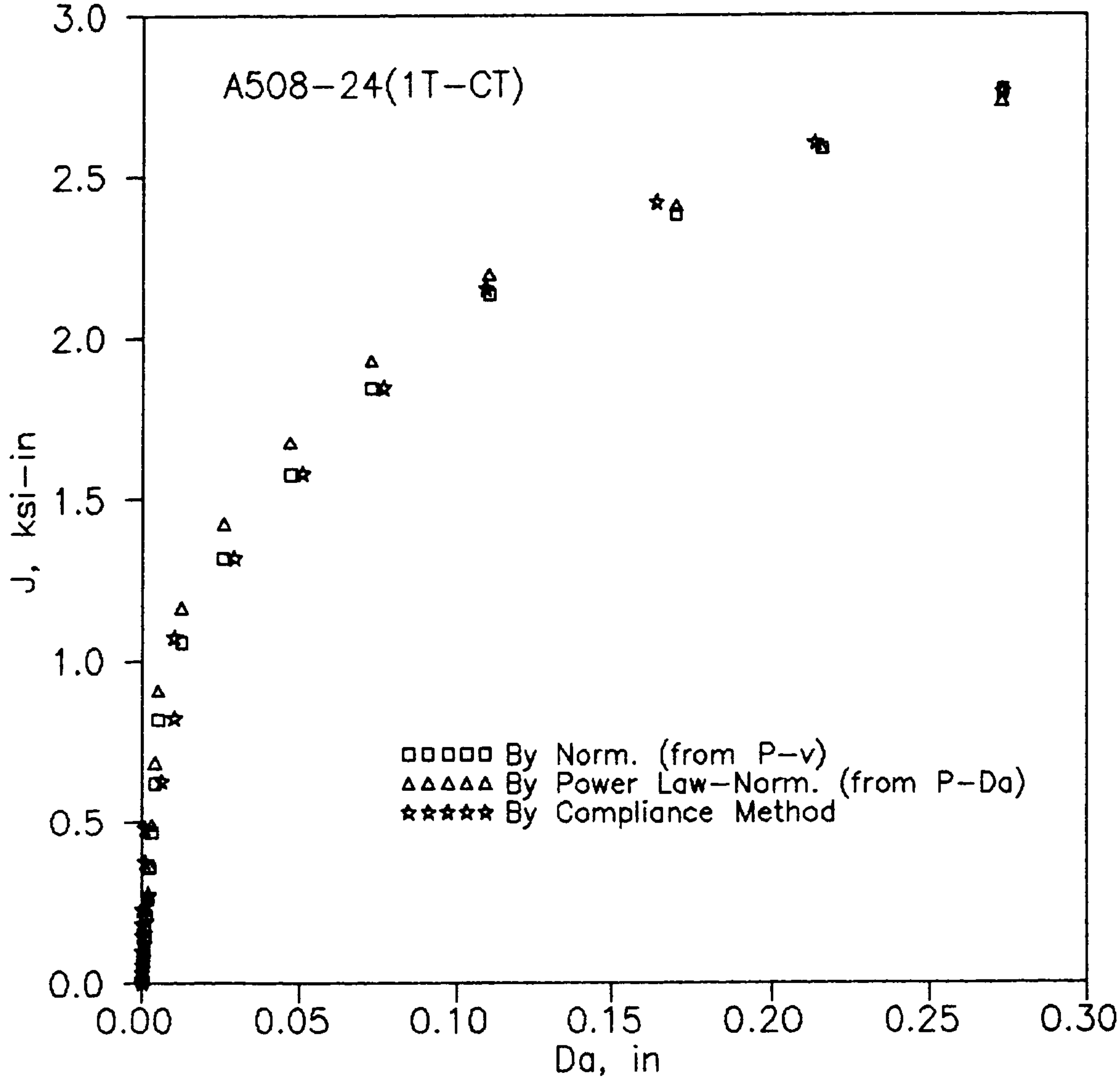

Fig. 39 J-R Curve from Power Law Approach for Specimen A508-24

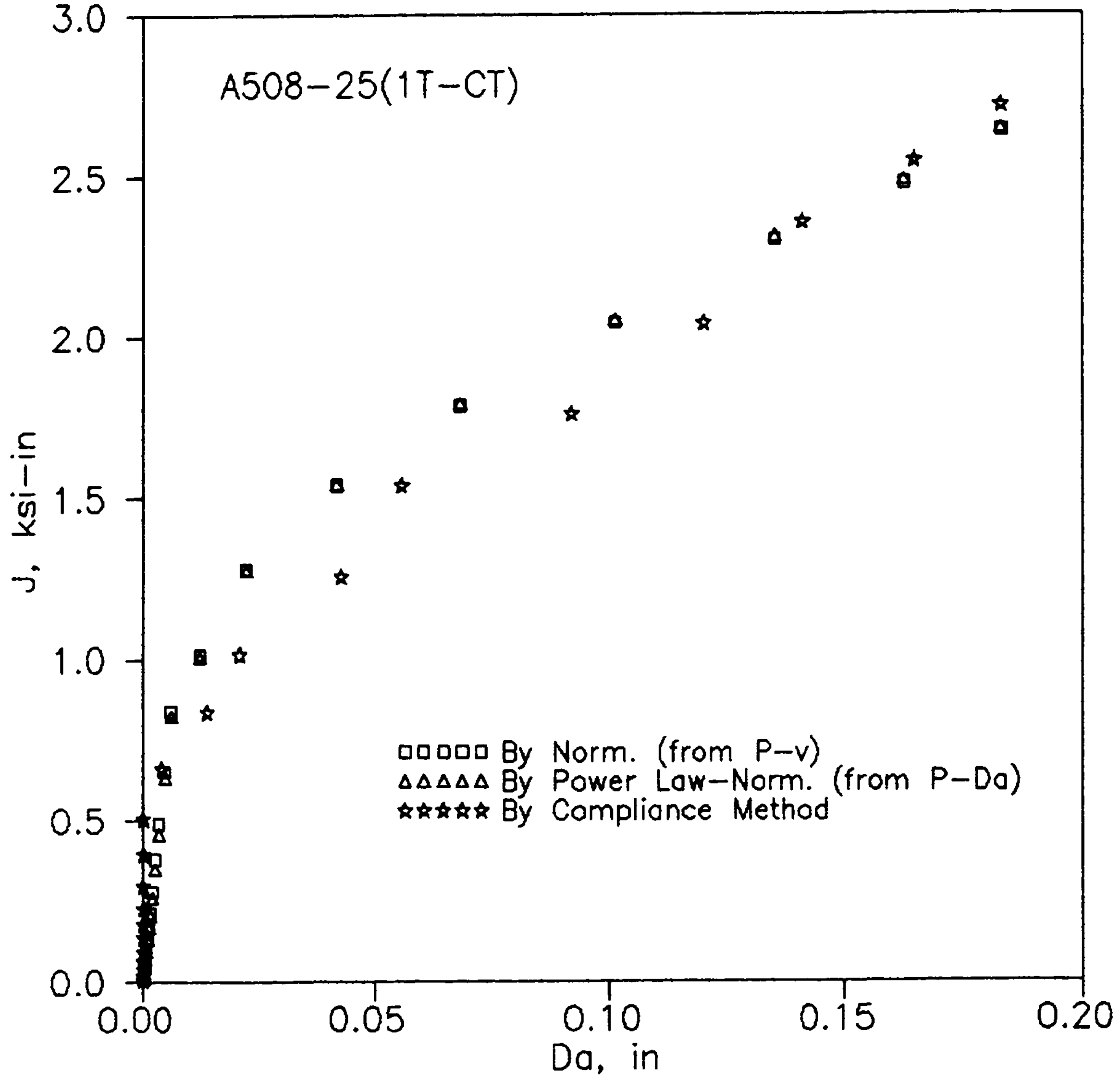

Fig. 40 J-R Curve from Power Law Approach for Specimen A508-25

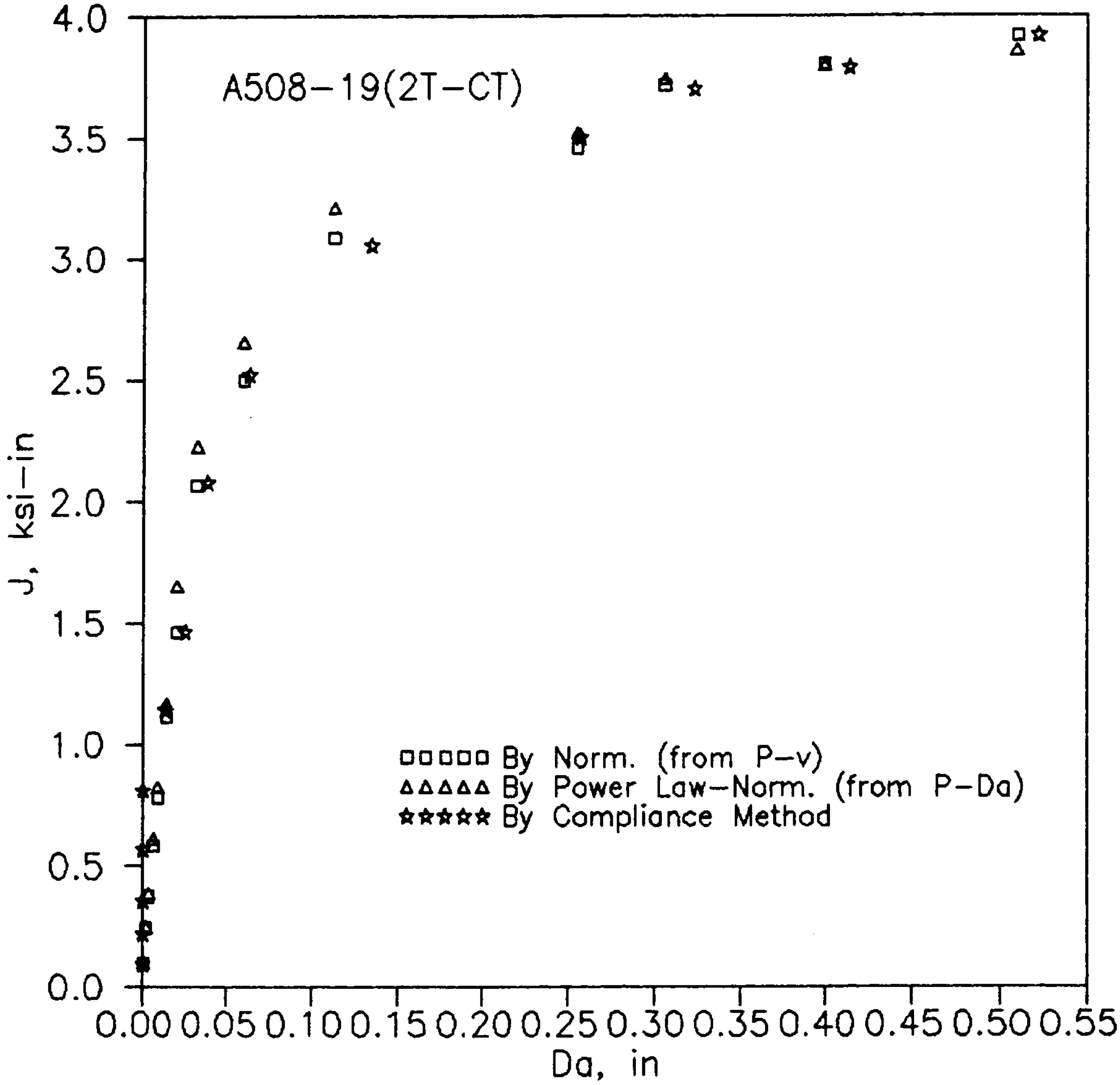

Fig. 41 J-R Curve from Power Law Approach for Specimen A508-19

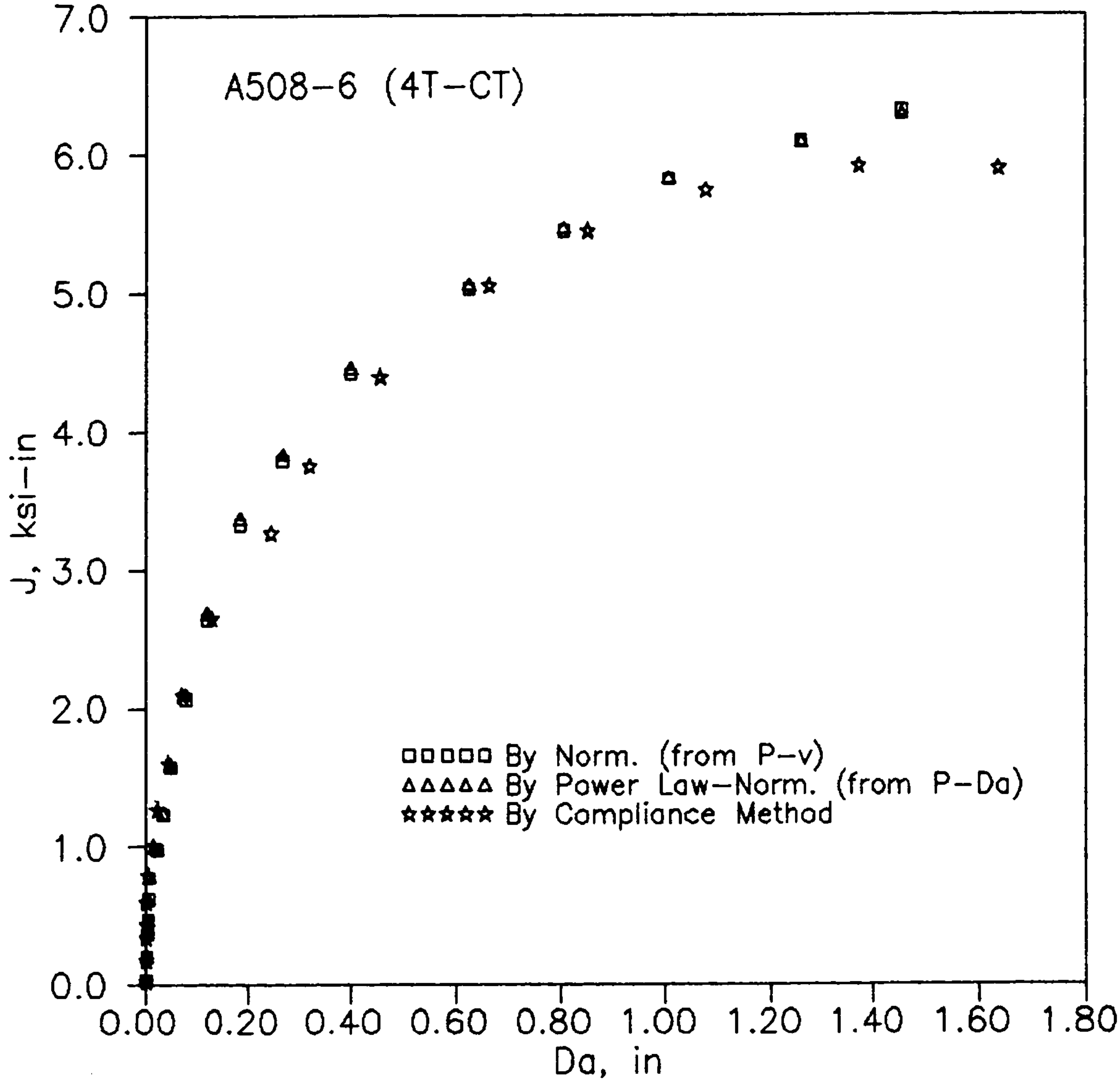

Fig. 42 J-R Curve from Power Law Approach for Specimen A508-6

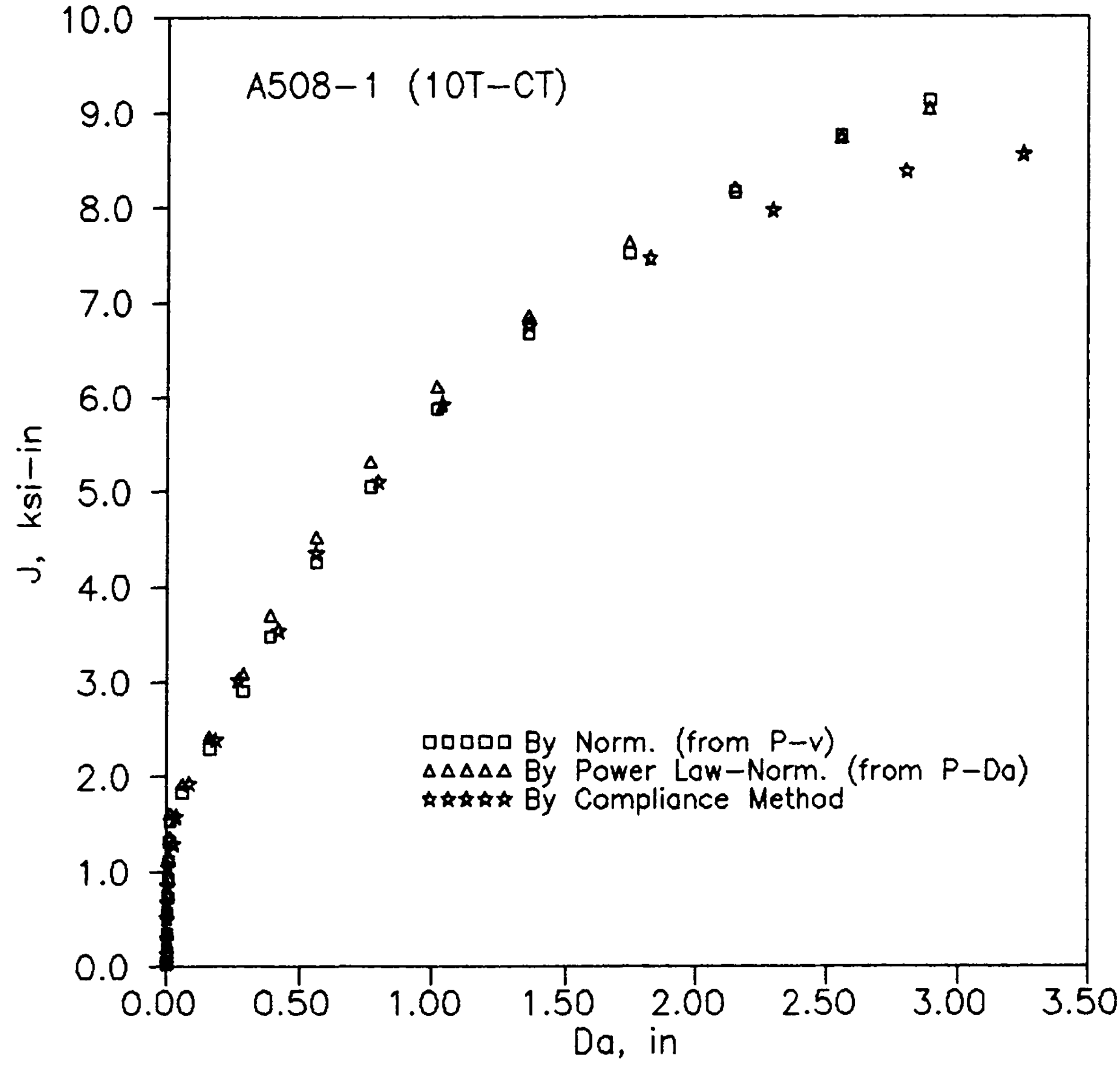

Fig. 43 J-R Curve from Power Law Approach for Specimen A508-1

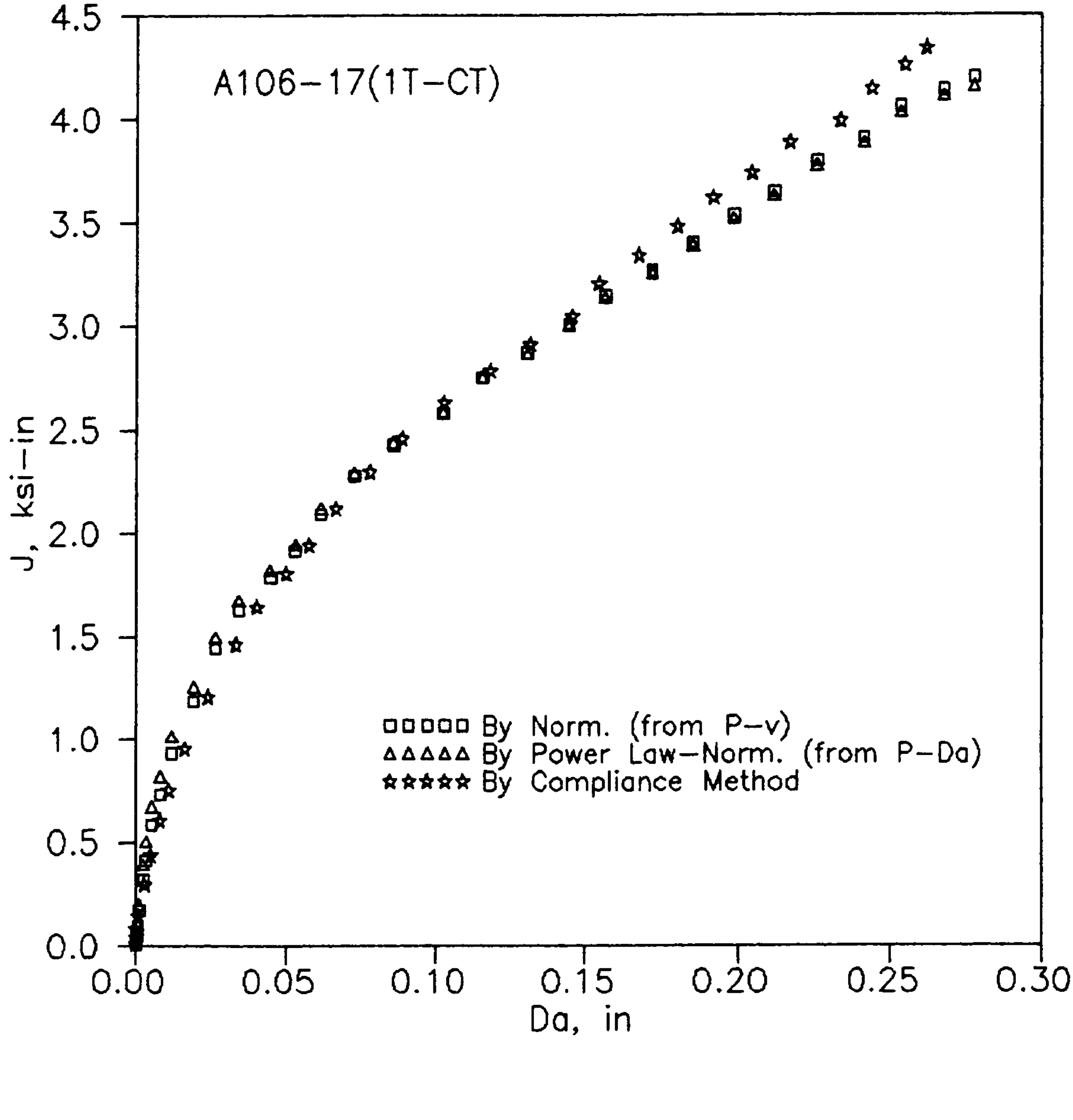

Fig. 44 J-R Curve from Power Law Approach for Specimen A106-17

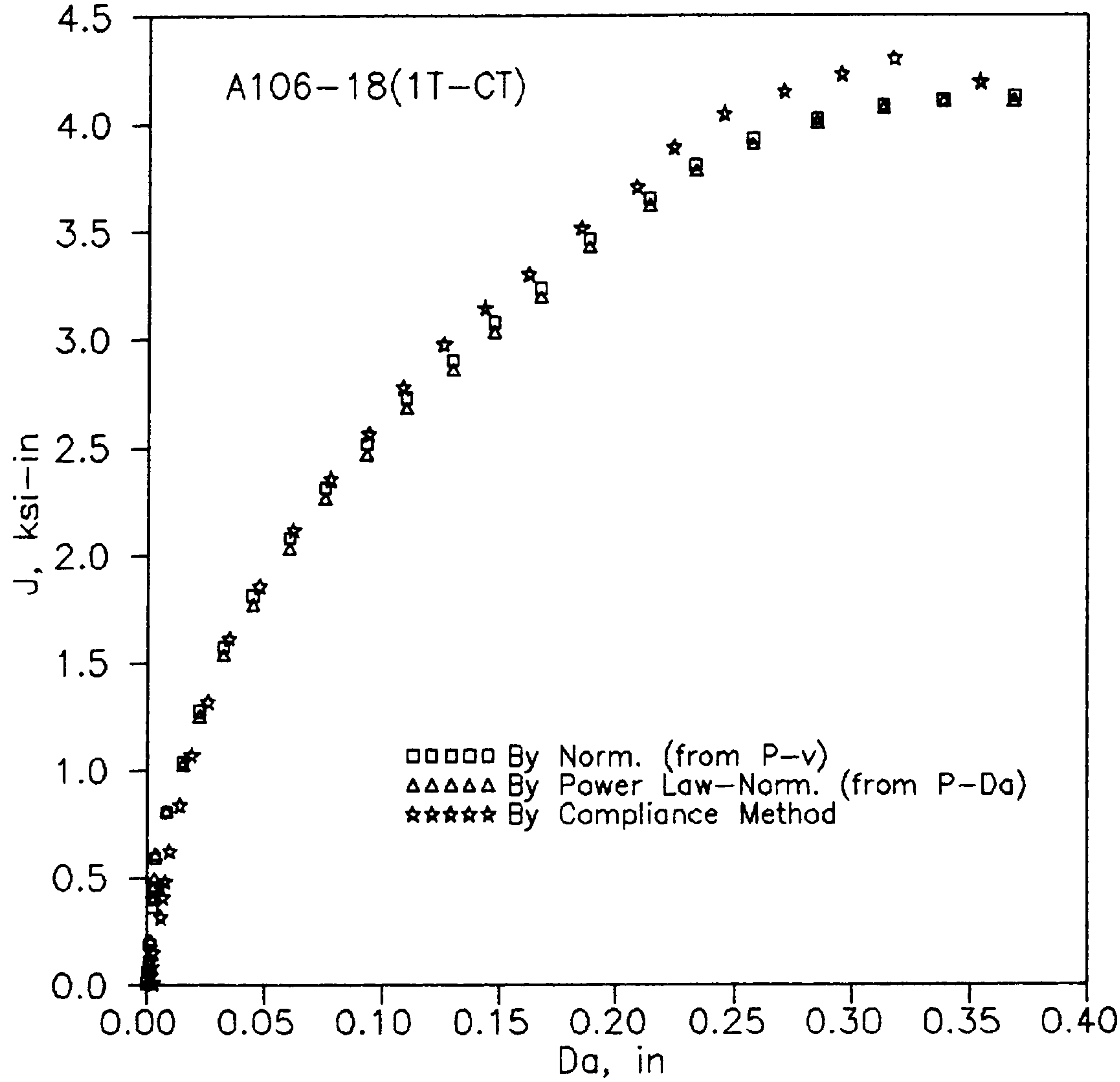

Fig. 45 J-R Curve from Power Law Approach for Specimen A106-18

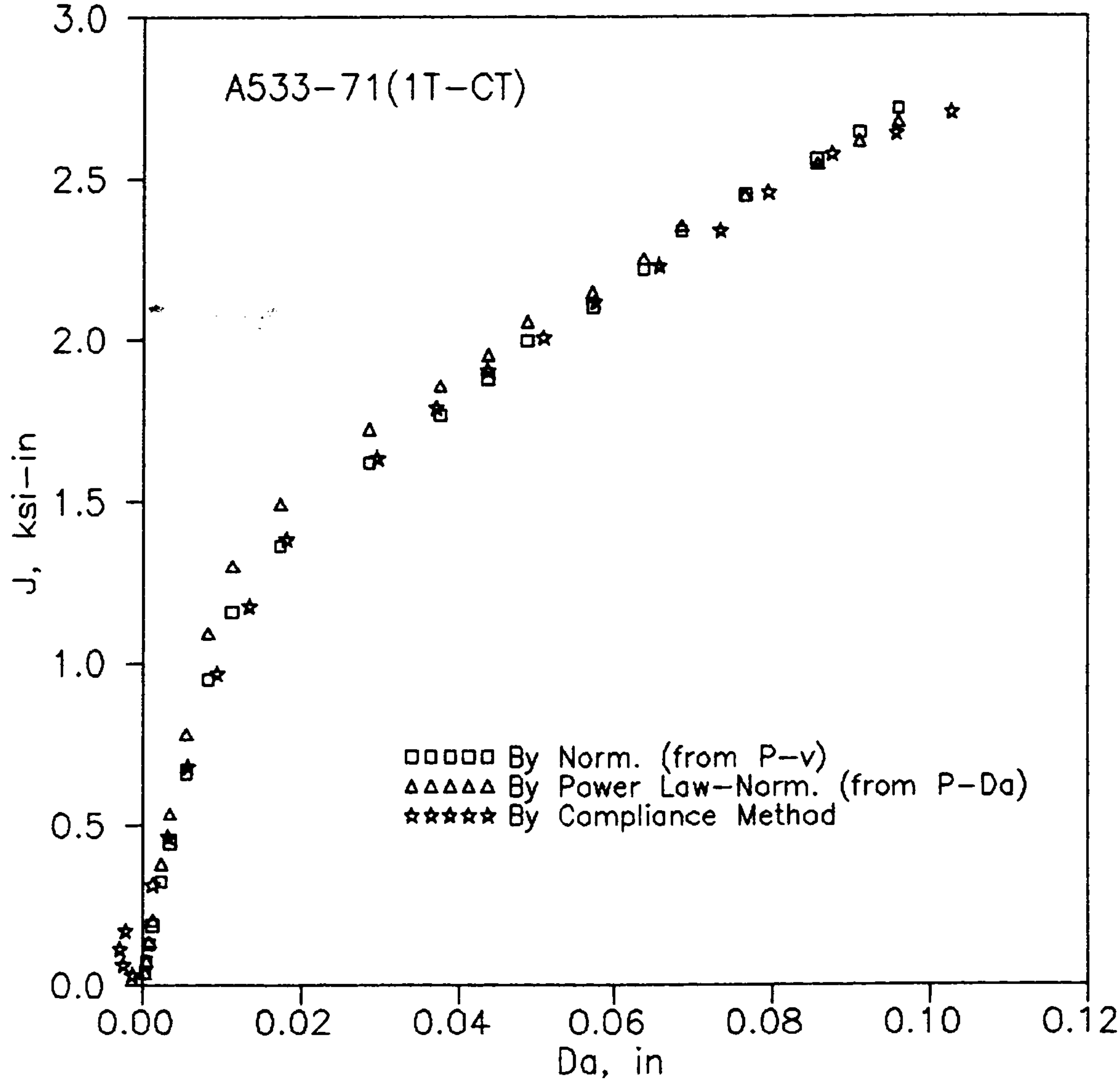

Fig. 46 J-R Curve from Power Law Approach for Specimen A533-71

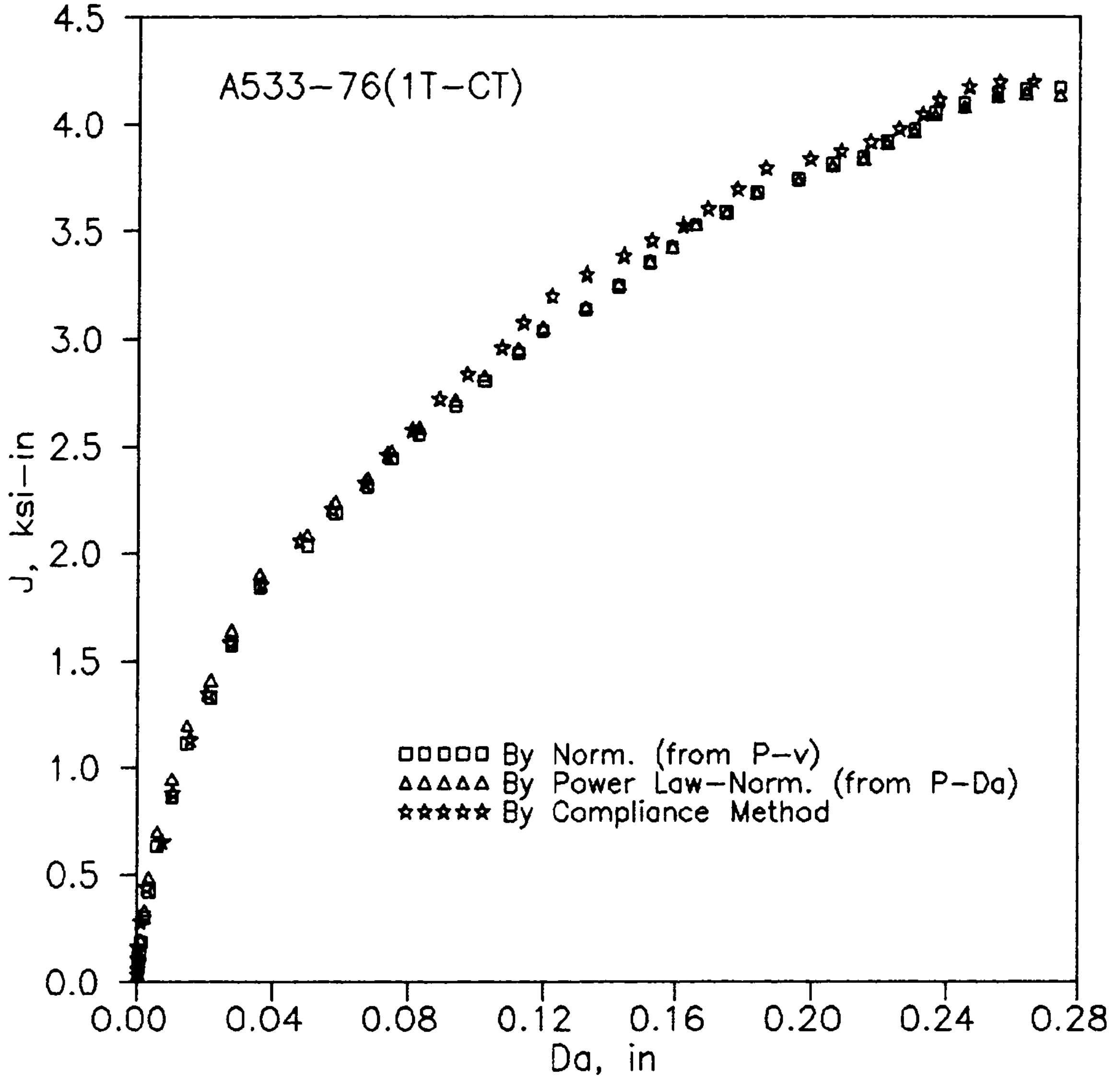

Fig. 47 J-R Curve from Power Law Approach for Specimen A533-76

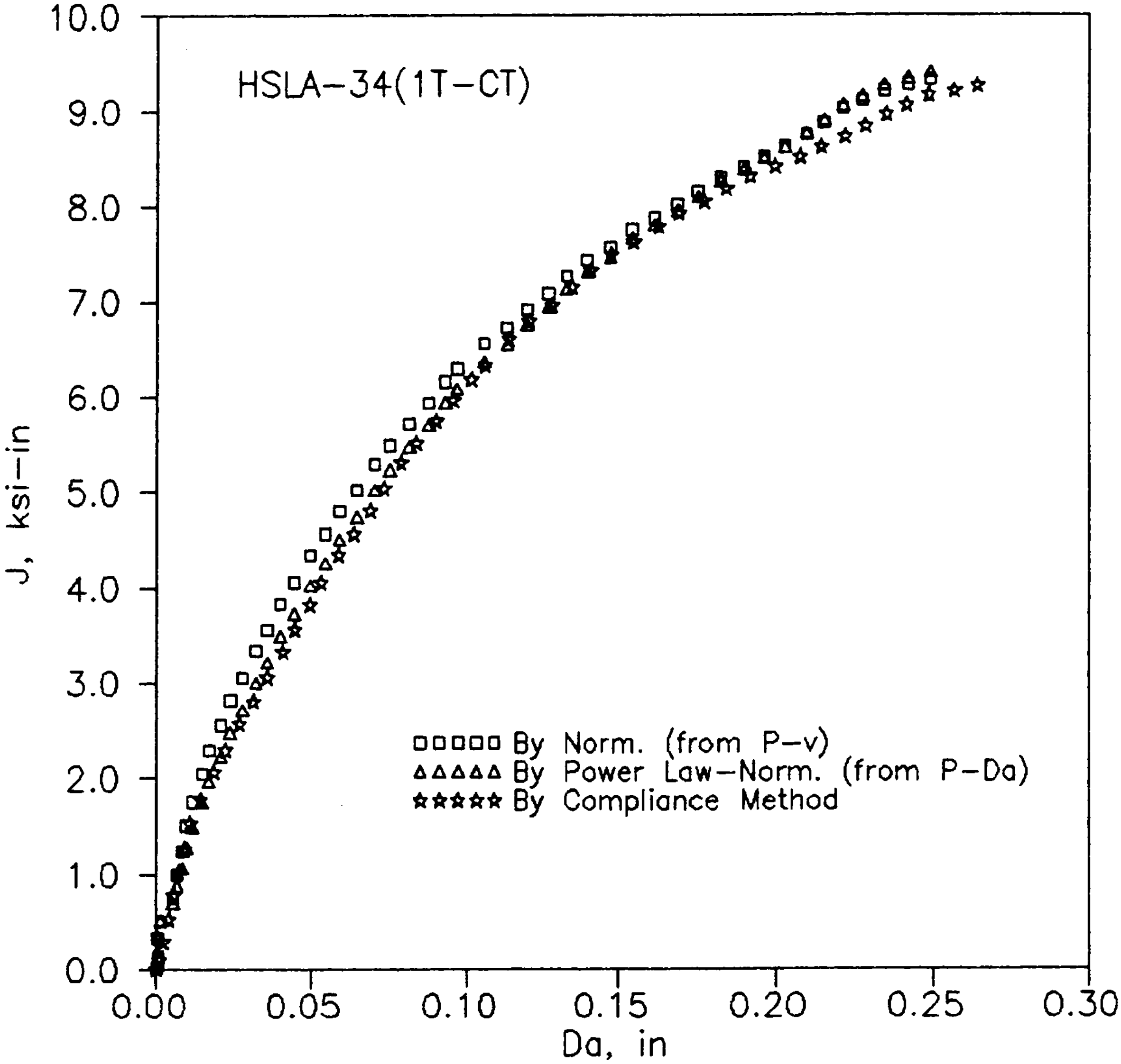

Fig. 48 J-R Curve from Power Law Approach for Specimen HSLA-34

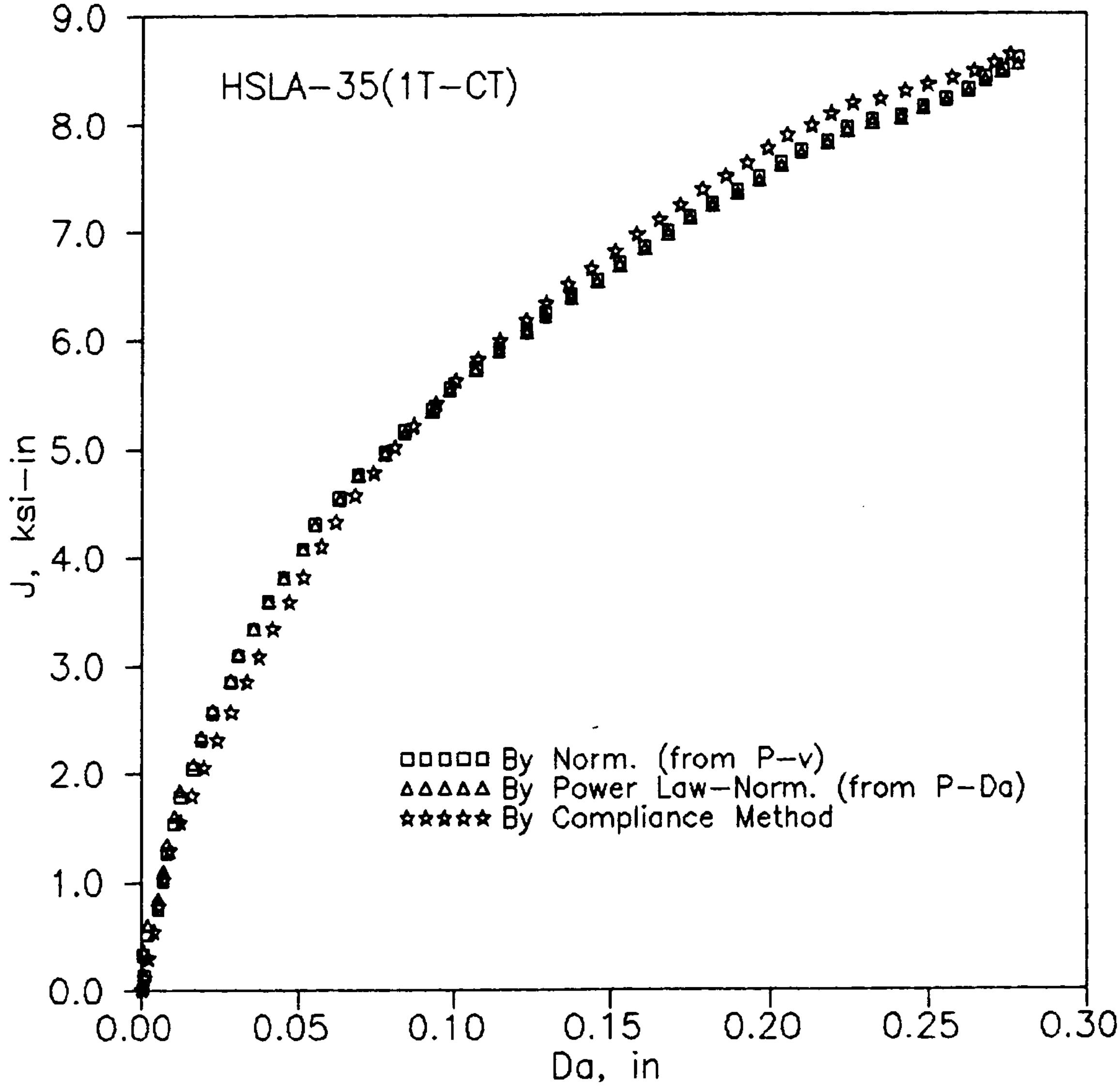

Fig. 49 J-R Curve from Power Law Approach for Specimen HSLA-35

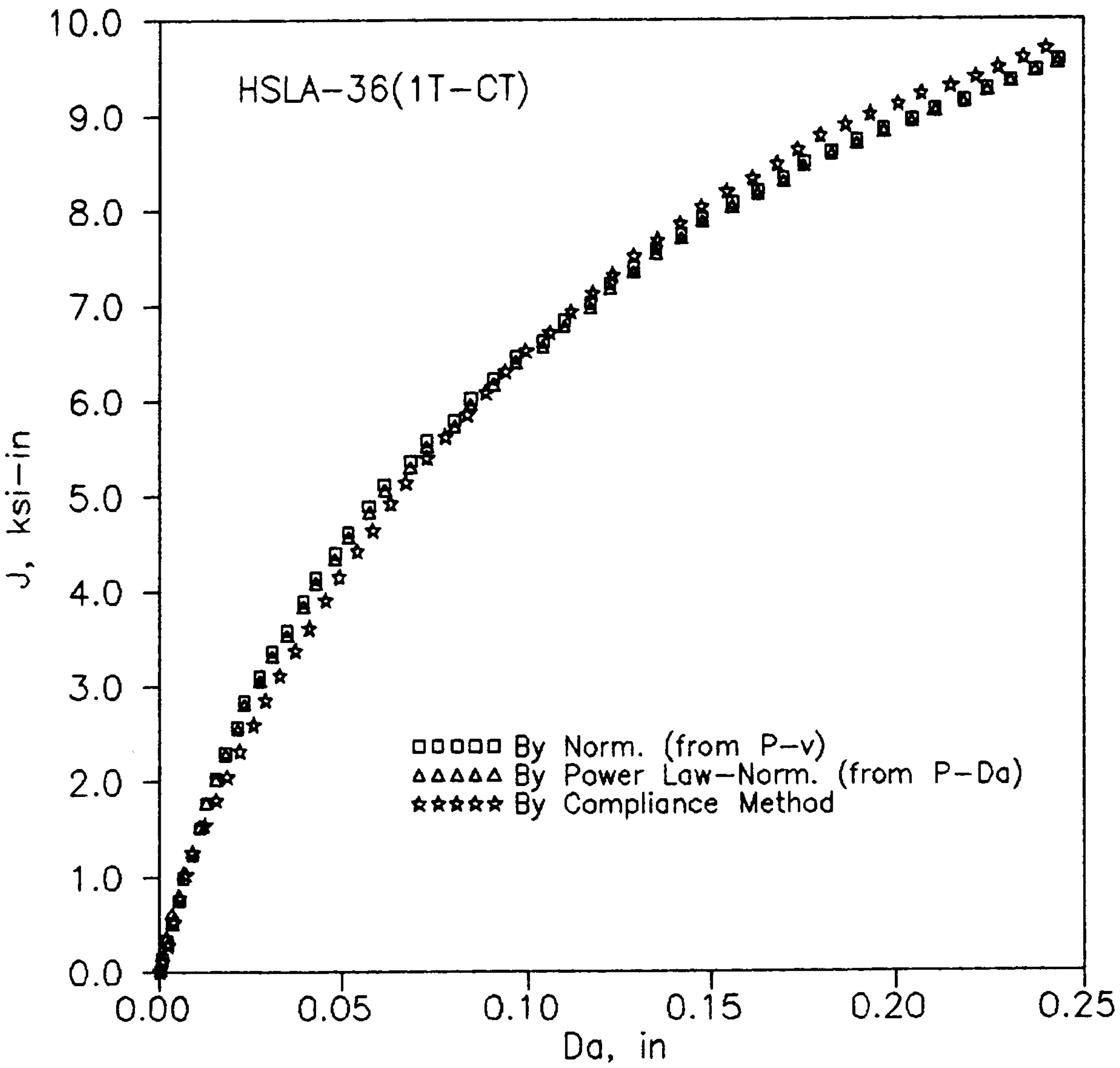

Fig. 50 J-R Curve from Power Law Approach for Specimen HSLA-36

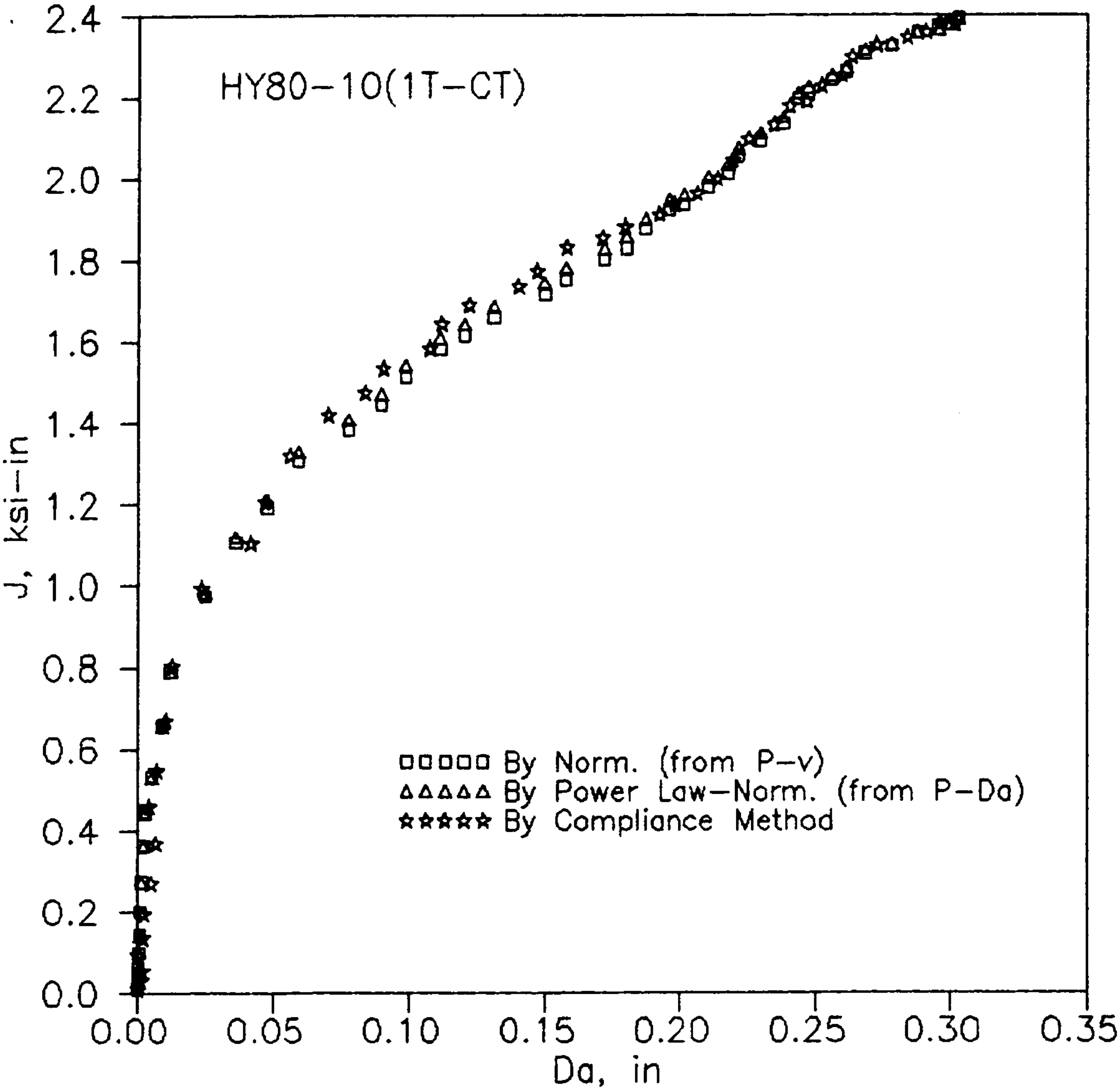

Fig. 51 J-R Curve from Power Law Approach for Specimen HY80-10

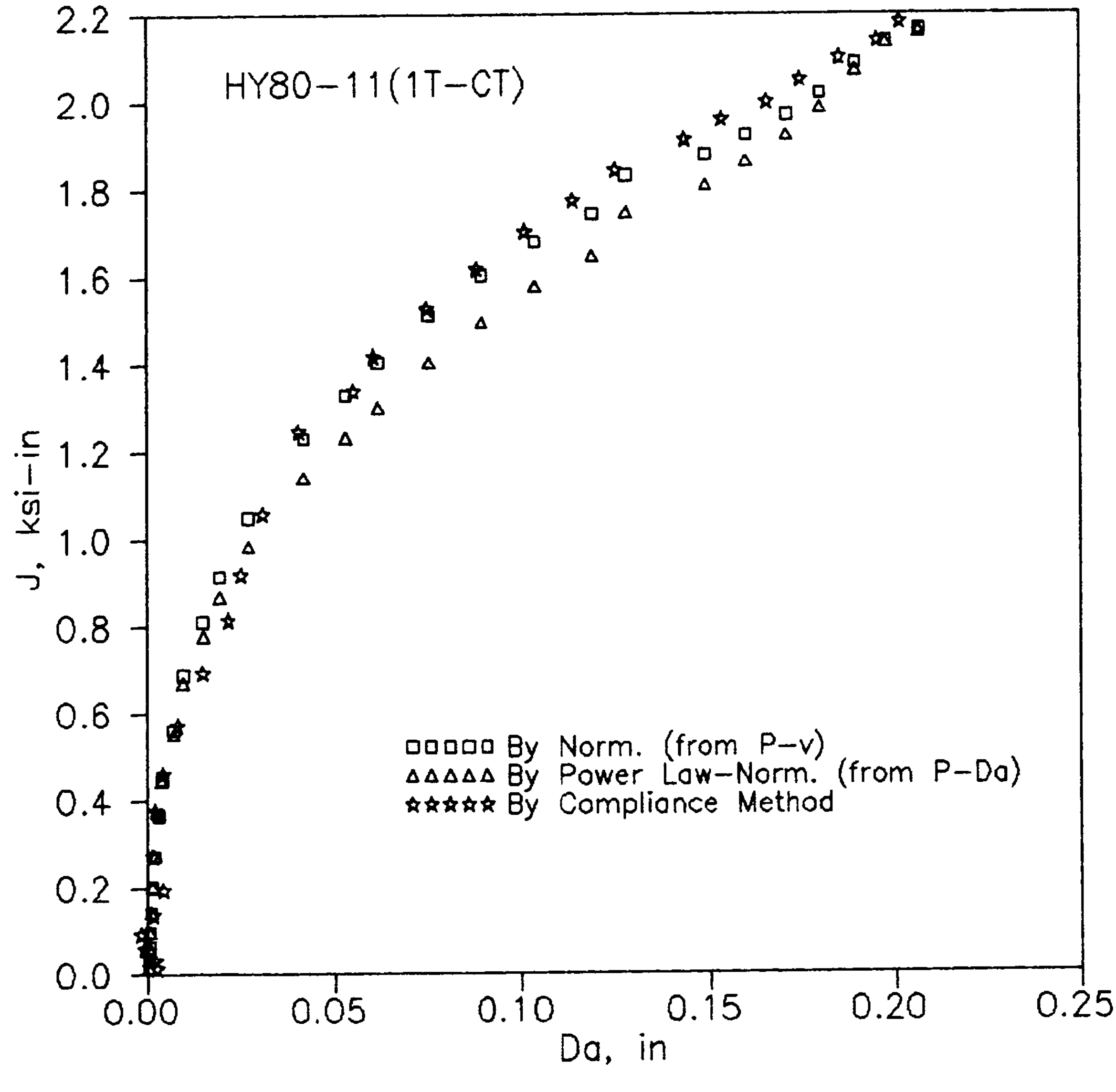

Fig. 52 J-R Curve from Power Law Approach for Specimen HY80-11

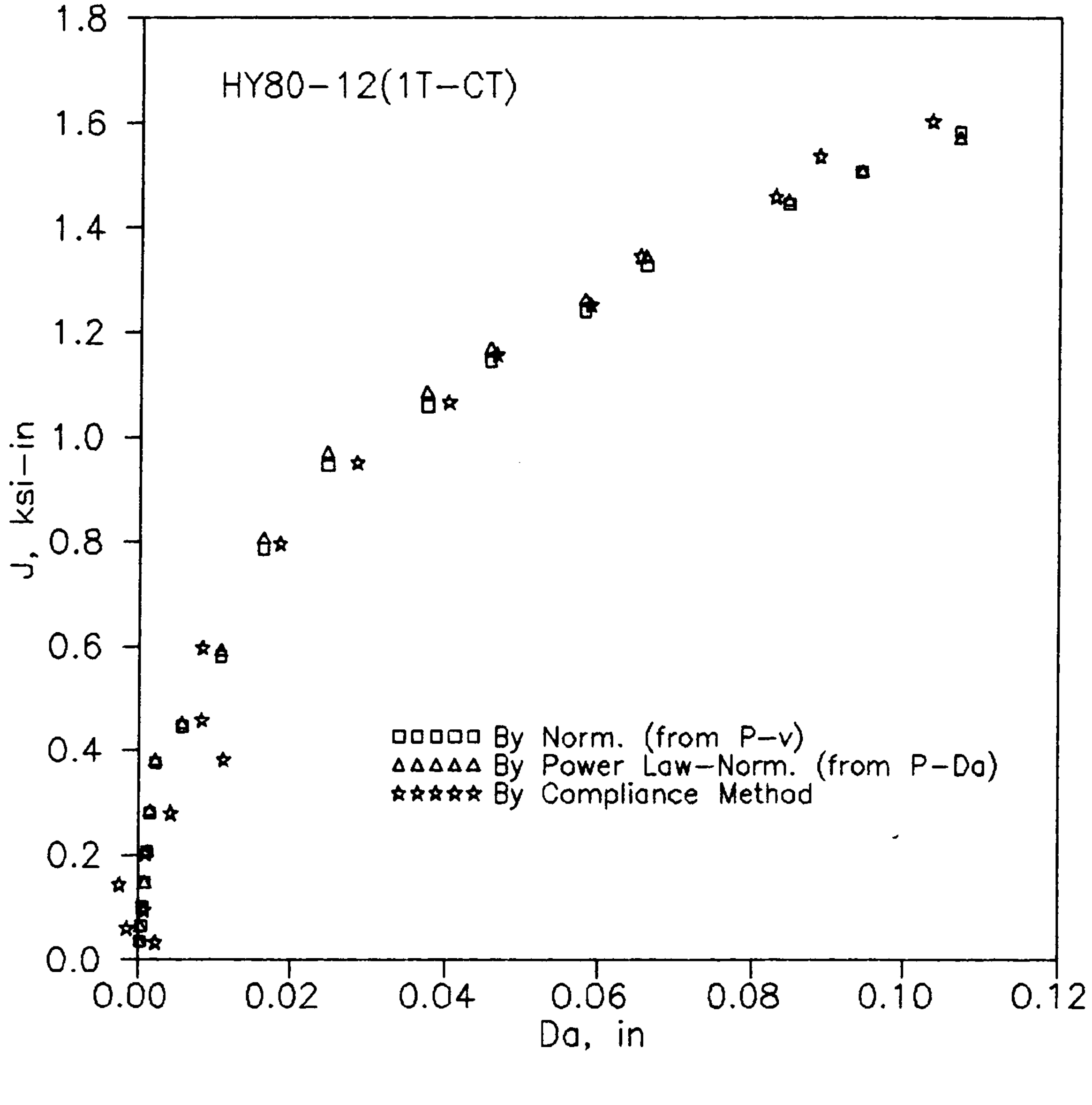

Fig. 53 J-R Curve from Power Law Approach for Specimen HY80-12

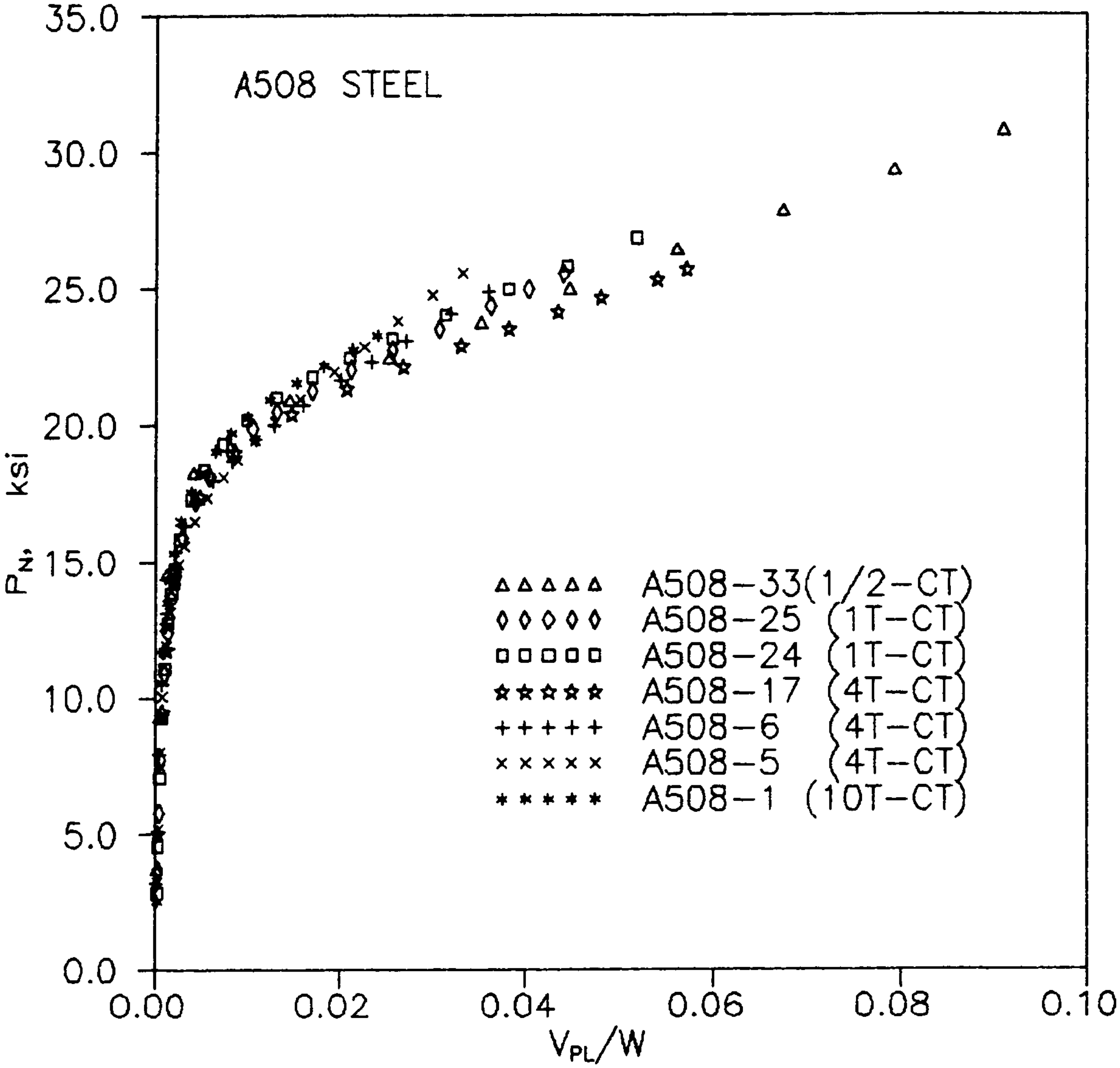

Fig. 54 **Normalized Deformation Curves for A508 Steel Specimens Showing They Have Almost Same Behaviors at the Beginning Region**

VITA

Kang Lee was born on May 2, 1946, in Kunming, Yunnan province, China. He attended elementary and high schools in that city and was graduated from the Eleventh High School of Kunming in September 1965. At that time , "the Cultural Revolution" had begun in China and all universities were closed. He could not continue to study and was employed by the Third Machine Manufacture Company of Kunming. He served as an assistant engineer in that company for 14 years. In January 1979 he got an opportunity to enter the Central Radio-Television University of China and received a B. S. degree in Mechanical Engineering in June 1982. After that he returned to the same Company and served as an engineer and the head of the Technical Department.

In November 1984 he came to United States and studied as a visiting scholar in the Engineering Science and Mechanics department of the University of Tennessee. In the spring quarter of 1988 he began to study toward a M. S. degree in the same department. When this degree is to be awarded in August 1990, he plans to continue in the Ph.D program of the same department.